

## Synthesis, Characterization and Optimization for *in Vivo* Delivery of a Non-Selective Isopeptidase Inhibitor as New Anti-Neoplastic Agent

Ulma Cersosimo,<sup>†#</sup> Andrea Sgorbissa,<sup>‡#</sup> Carmen Foti,<sup>‡</sup> Sara Drioli,<sup>†</sup> Rosario Angelica,<sup>‡</sup> Andrea Tomasella,<sup>‡</sup> Raffaella Picco,<sup>‡</sup> Marta Stefania Semrau,<sup>§</sup> Paola Storici,<sup>§</sup> Fabio Benedetti,<sup>†</sup> Federico Berti,<sup>\*†</sup> and Claudio Brancolini<sup>\*‡</sup>

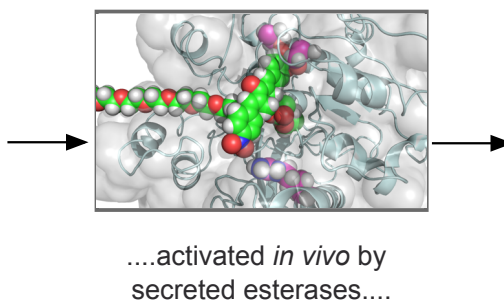
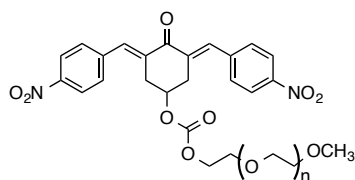
<sup>†</sup>Dipartimento di Scienze Chimiche e Farmaceutiche, Università degli Studi di Trieste. Via Giorgieri 1 – 34127 Trieste ITALY.

<sup>‡</sup>Dipartimento di Scienze Mediche e Biologiche Università degli Studi di Udine. P.le Kolbe 4 - 33100 Udine ITALY.

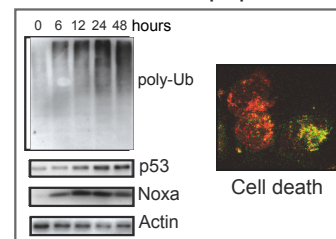
<sup>§</sup>Structural biology laboratory, Elettra - Sincrotrone Trieste S.C.p.A., Area Science Park, Basovizza, 34149 Trieste, Italy

### ABSTRACT

A Non-Selective Isopeptidase Inhibitor....



.... that inhibits the UPS and induces apoptosis



Bis arylidenecycloalkanones structurally related to the Non Selective Isopeptidase Inhibitor G5 were synthesized and tested for cytotoxic activity against glioblastoma cells. Cytotoxicities correlate well with Hammett  $\sigma$  constants for substituted arylidene groups confirming the proposed inhibition mechanism. A new inhibitor (**2c**) based on the 4-hydroxycyclohexanone scaffold, that favors apoptosis over necrosis, was selected for further development. **2c** inhibited representative deubiquitinases with micromolar  $IC_{50}$  and its pro-apoptotic activity was studied on several cancer cell lines. Inhibitor **2c** was conjugated to PEG via dicarbammate and diester linkers. While the dicarbammate was inactive, the diester (**2cPE**) behaves like a pro-drug and is converted into the active species **2c** by secreted esterase activities. Finally, **2cPE** was also tested *in vivo*, on A549 lung carcinoma xenografts generated in mice. Intravenous treatment with **2cPE** led to a significant reduction in primary tumor growth, without appreciable toxicity to mice.

## INTRODUCTION

Protein modification by the addition of the 8-kDa Ubiquitin or Ub-like proteins is a well known and widespread post-translation modification not limited to influencing protein destruction, but also their subcellular localization or the assembling into multi-proteins complexes.<sup>1-3</sup> Ub and Ubl peptides are generally ligated to proteins by the sequential action of three enzymes: an ubiquitin-activating enzyme (E1), an Ub-carrier enzyme (E2) and an Ub-protein ligase (E3). E3 enzymes show specificity in substrate choice and represent critical players in several signaling pathways.<sup>3,4</sup>

Ub and Ubl-linkages are reversible and their cleavage entails on the involvement of a large family of enzymes, known as isopeptidases. Although isopeptidases can be viewed as E3-ligase antagonists, additional functions, such as maturation of Ub or Ubl peptides, are under their supervision. The isopeptidase family includes deubiquitinating enzymes (DUBs), which in principle should be specifically devoted to the rupture of Ub-linkages, and other proteolytic enzymes, which target additional Ubl-proteins.<sup>5,6</sup>

The discovery of bortezomib<sup>7</sup> and its approval for the treatment of relapsed multiple myeloma and mantle cell lymphoma has open the field to new inhibitors targeting, more specifically, critical enzymes of the ubiquitin-proteasome system (UPS) and showing less adverse side effects.<sup>8,9</sup> In this scenario E3 ligases and DUBs/isopeptidases have gained increasing attention as targets for drug development. These enzymes represent good candidates to influence the function of proteins controlling the transformed phenotype or to induce cellular stresses, which can kill cancer cells.<sup>9-12</sup>

In the last decade several reports have described the discovery, synthesis and characterization of isopeptidase inhibitors.<sup>13-23</sup> Based on the specific target selectivity, they can be divided in two classes: selective inhibitors, acting on a specific enzyme or on a limited number of enzymes, and non-selective isopeptidase inhibitors (N-SIIs), which in principle can affect the activity of several isopeptidases. The two classes offer different and complementary advantages for the development of new anticancer treatments. The first class guarantees advantages in terms of selectivity when growth/survival of a specific tumor depends on a specific isopeptidase. On the other hand, the second class, affecting more enzymes and multiple pathways, may offer advantages in terms of effectiveness on different tumors. Hence, further studies to improve the anti-neoplastic activities of inhibitors of both classes are of primary importance.

A subclass of N-SIIs brings together molecules characterized by the presence of a cross-conjugated  $\alpha,\beta$ -unsaturated dienone with two sterically accessible electrophilic  $\beta$ -carbons<sup>13</sup> that can act as Michael acceptors to target nucleophiles, like the catalytic cysteine of several isopeptidases.<sup>13-17</sup> Recently, a molecule of this family, RA190, has been engineered to exert specificity against proteasome ubiquitin receptor RPN13 (Figure 1).<sup>23</sup>

Optimization of these inhibitors in terms of *in vivo* efficacy is a fundamental step towards their possible use in the clinic. In this work, starting from G5, a N-SII previously identified by us (Figure 1),<sup>14</sup> we performed structure-activity studies that lend support to the proposed mechanism of inhibition and allowed us to develop a G5-derivative optimized for *in vivo* anti-neoplastic activity.

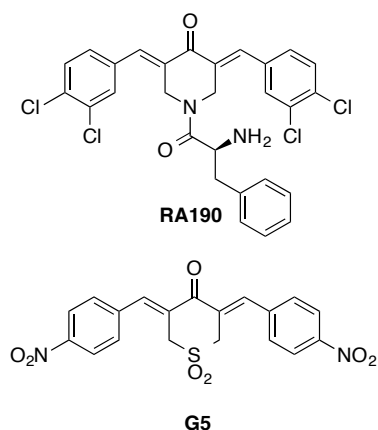
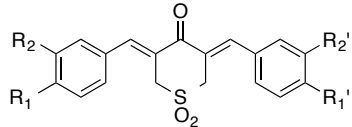


**Figure 1.** Cross-conjugated dienone N-SIIs RA190 and G5

## RESULTS AND DISCUSSION

**Structure-activity studies.** The effect on tumor cell survival of two series of dienones was investigated in glioblastoma U87MG cells, which in response to G5 enter both apoptosis and necrosis.<sup>24</sup> The first series (Table 1) is based on the bis(arylidene)-tetrahydrothiapyran-4-one-1,1-dioxide scaffold of G5 with variations in the substituents on the aromatic rings. In the second series (Table 2), the sulfone group of the G5 scaffold is replaced by other groups, while the 4-nitro substituents on the aromatic rings are fixed.

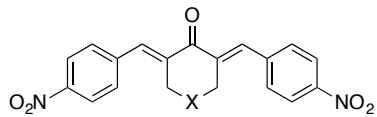
**Table 1.** Cytotoxicity of bis(arylidene)-tetrahydrothiapyran-4-one-1,1-dioxides against U87MG glioblastoma cells.



Compound	R <sub>1</sub>	R <sub>1</sub> '	R <sub>2</sub>	R <sub>2</sub> '	IC <sub>50</sub> [μM] <sup>a,b</sup>	s.d. <sup>b</sup>
<b>1a</b>	H	H	H	H	5.11	1.67
<b>1b</b>	CH <sub>3</sub>	CH <sub>3</sub>	H	H	4.74	0.21
<b>1c</b>	OH	OH	H	H	6.73	0.15
<b>1d</b>	OCH <sub>3</sub>	OCH <sub>3</sub>	H	H	3.57	0.72
<b>1e</b>	OPh	OPh	H	H	2.94	0.57
<b>1f</b>	F	F	H	H	2.21	0.23
<b>1g</b>	CN	CN	H	H	1.35	0.15
<b>1h</b>	OCH <sub>3</sub>	OCH <sub>3</sub>	NO <sub>2</sub>	NO <sub>2</sub>	1.14	0.18
<b>1i</b>	H	H	NO <sub>2</sub>	NO <sub>2</sub>	0.76	0.07
<b>1j</b>	NO <sub>2</sub>	OH	H	H	2.17	0.27
<b>1k</b>	NO <sub>2</sub>	OCH <sub>3</sub>	H	H	2.09	0.42
<b>1l</b>	NO <sub>2</sub>	CH <sub>3</sub>	H	H	1.39	0.34
<b>G5</b>	NO <sub>2</sub>	NO <sub>2</sub>	H	H	0.77	0.21

<sup>a</sup> From cell viabilities measured with a resazurin assay, 48 hours after treatments. <sup>b</sup> Experiments were carried out in triplicate and are presented as mean values and standard deviations (s.d.).

**Table 2.** Cytotoxicity of nitrobenzylidene dienones against U87MG glioblastoma cells.

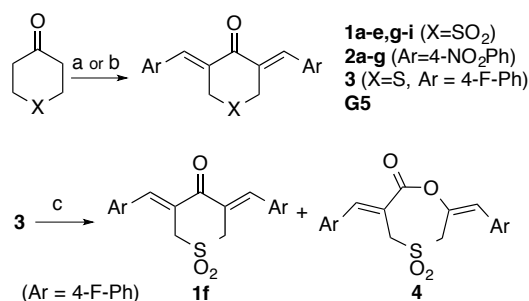


Compound	X	IC <sub>50</sub> [μM] <sup>a,b</sup>	s.d. <sup>b</sup>
<b>2a</b>	CH <sub>2</sub>	27.5	2.0
<b>2b</b>	CH(OCH <sub>2</sub> CH <sub>2</sub> O)	15.33	0.71
<b>2c</b>	CHOH	4.62	1.96
<b>2d</b>	CHCOOC <sub>2</sub> H <sub>5</sub>	2.47	0.25
<b>2e</b>	NH	7.15	2.90
<b>2f</b>	O	50.1	14.3
<b>2g</b>	S	11.6	2.01
<b>2h</b>	SO	1.79	0.81
<b>G5</b>	SO <sub>2</sub>	0.77	0.21

<sup>a</sup> From cell viabilities measured with a resazurin assay, 48 hours after treatments. <sup>b</sup> Experiments were carried out in triplicate and are presented as mean values and standard deviations (s.d.).

With the exception of the fluoro derivative **1f**, symmetrical compounds **1a-i** and **G5** were obtained by the acid catalyzed Knoevenagel condensation of tetrahydrothiapyran-4-one-1,1-dioxide (Scheme 1, X = SO<sub>2</sub>) with aromatic aldehydes.<sup>25,26</sup> An alternative approach was adopted for the synthesis of **1f** (scheme 1), consisting in the condensation between the corresponding aldehyde and tetrahydrothiapyran-4-one followed by mCPBA oxidation of the resulting sulfide **3**. The oxidation of the p-fluoro derivative **3** to the desired sulfone **1f** was accompanied by the formation of the Baeyer-Villiger by-product **4** (Scheme 1). The two products, in ratio 3 : 1, were easily separated by crystallization from acetone/hexane.

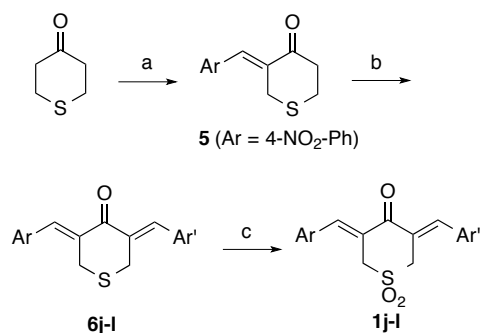
**Scheme 1.** Synthesis of symmetrical derivatives of series 1 and 2<sup>a</sup>



<sup>a</sup>Reagents and conditions: (a) ArCHO, EtOH, aq. HCl, 15-78 %; (b) ArCHO, EtOH, Ba(OH)<sub>2</sub>, 52% (for **2b**); (c) mCPBA, CH<sub>2</sub>Cl<sub>2</sub>, 41-63%.

Unsymmetrical compounds **1j-l** were obtained as shown in Scheme 2. Tetrahydrothiapyran-4-one was initially converted into the mono-alkylidene derivative **5** by an aldol reaction with 4-nitrobenzaldehyde followed by dehydration of the aldol. Acid-catalyzed Knoevenagel reaction of **5** with the appropriate aromatic aldehyde was then followed by mCPBA oxidation of the sulfides **6j-l**.

**Scheme 2.** Synthesis of unsymmetrical derivatives of series 1<sup>a</sup>



<sup>a</sup>Reagents and conditions: (a) (i) ArCHO, NaOH, MgSO<sub>4</sub>, H<sub>2</sub>O, (ii) HCl, EtOH 56%; (b) ArCHO, EtOH, aq. HCl, 44-95%; (c) mCPBA, CH<sub>2</sub>Cl<sub>2</sub>, 21-90%.

All compounds of series 2 (Table 2) are symmetrical and, with the exception of **2h**, were obtained by the Knoevenagel condensation of the appropriate ketone and 4-nitrobenzaldehyde (Scheme 1). For compound **2b**, containing an acid-labile acetal group, the condensation was carried out in basic conditions.<sup>27</sup> Sulfoxide **2h** (Table 2) was obtained by mCPBA oxidation of the corresponding sulfide **2g**. Even under controlled conditions (1 eq. mCPBA, 0 °C) the reaction gave a 1 : 1 mixture of sulfoxide **2h** and sulfone **G5**, but the desired product **2d** was readily purified by flash chromatography on silica gel.

<sup>1</sup>H- and <sup>13</sup>C-NMR spectroscopy showed that all compounds of series 1 and 2 were single stereoisomers with the aryl groups *trans* with respect to the carbonyl.

Data in Table 1 indicate that all the sulfones of series 1 are active against U87MG glioblastoma cells with  $IC_{50}$  values in the range 0.8-7 $\mu$ M, the dinitroderivatives **G5** and **1i** being the most active compounds of the series. Variations of hydrophobicity (logP values) and solvent accessible area are small in this series, reflecting the limited structural changes, and no general correlation is observed between these parameters and cytotoxicity. However, a clear correlation can be observed between cytotoxicity and the electronic effect of the substituents on the aromatic ring. A plot of the logarithm of the observed  $IC_{50}$  against the sum of the Hammett  $\sigma$  constants for the substituents on the aromatic rings<sup>28</sup> (Figure 2) reveals that cytotoxicity depends on the electron-withdrawing ability of the substituents, suggesting that the cytotoxic activity is directly related to the electrophilicity of the enone  $\beta$ -carbon. This is consistent with the observation that alcohol **7**, obtained by  $NaBH_4$  reduction of **G5**, is devoid of any cytotoxic activity and strongly suggests that cytotoxicity may indeed result from the alkylation of cysteine residues present in the catalytic site of isopeptidases by the dienone moiety.<sup>13,29</sup> Similar correlations have been observed also for cytotoxic N-acyl-bis(arylidene)-4-piperidones,<sup>30</sup> and arylidenecyclohexanones,<sup>31,32</sup> which have been postulated to selectively react as Michael acceptors with cellular thiols.<sup>29</sup>

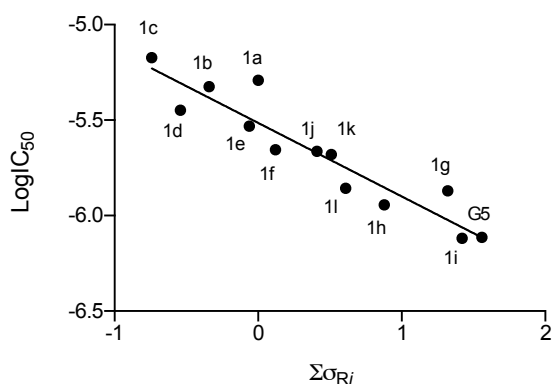
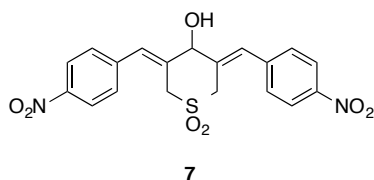


**Figure 2.** Linear correlation between U87MG glioblastoma cells cytotoxicity ( $LogIC_{50}$ ) and Hammett  $\sigma$  constants for compounds of series 1 (slope:  $-0.39 \pm 0.04$ ;  $r^2$ : 0.8808).  $\Sigma\sigma_{Ri}$  is the sum of the  $\sigma_p$  and/or  $\sigma_m$  for all the substituents on both rings.



Finally, the contribution of the X group was investigated in a series of di-nitro derivatives **2** (Table 2). While all compounds in this series are cytotoxic, the presence of a polar, electron withdrawing group in the six-membered ring appears in general to be beneficial to achieve strong activity.

**Assessment of the dienones-induced apoptotic and necrotic responses.** In cells resistant to apoptosis, such as mouse fibroblasts defective for Bax and Bak (Bax/Bak DKO) or glioblastoma U87MG cells, **G5** can also activate a caspase-independent death.<sup>24,33</sup> Although caspase-independent death can engage different mechanisms, previous studies have excluded the involvement of autophagy (Foti et al., 2009, Autophagy 5:4, 1-3) and have demonstrated that **G5** triggers a necrotic cell death.<sup>33,34</sup> Hence, we decided to study, on a small set of dienones and using **G5** as a reference, whether variations in the structure affect the pro-necrotic and pro-apoptotic activities (Figure 3). To this purpose, we selected derivatives, **1b**, **2c** and **2h** and also used T98G glioblastoma cells, which preferentially die by apoptosis in response to **G5** (Figure 3).<sup>24,34</sup>

As illustrated in Figure 3 (A, B) the sulfoxide **2h** behaves similarly to **G5**, while compounds **1b** and **2c** show a higher propensity to trigger apoptosis compared to **G5** and **2h**. In fact, unlike the latter compounds, **1b** and **2c** are more effective in killing T98G than U87MG cells, as proved by trypan blue staining and caspase activities. Cell death in T98G cells, induced by **1b** and **2c**, is characterized by a robust caspase engagement. On the other side in

U87MG cells, during cell death induced by G5 and **2h**, caspases are much less involved, thus testifying to the existence of two different types of cell death. The differential induction of necrosis and apoptosis in the two cell lines was confirmed, for **2c**, by using the caspase inhibitor zVAD-fmk (Figure 3C), which was effective in counteracting cell death only in T98G cells; similar results were obtained with the other compounds (Supplementary Figure S1).

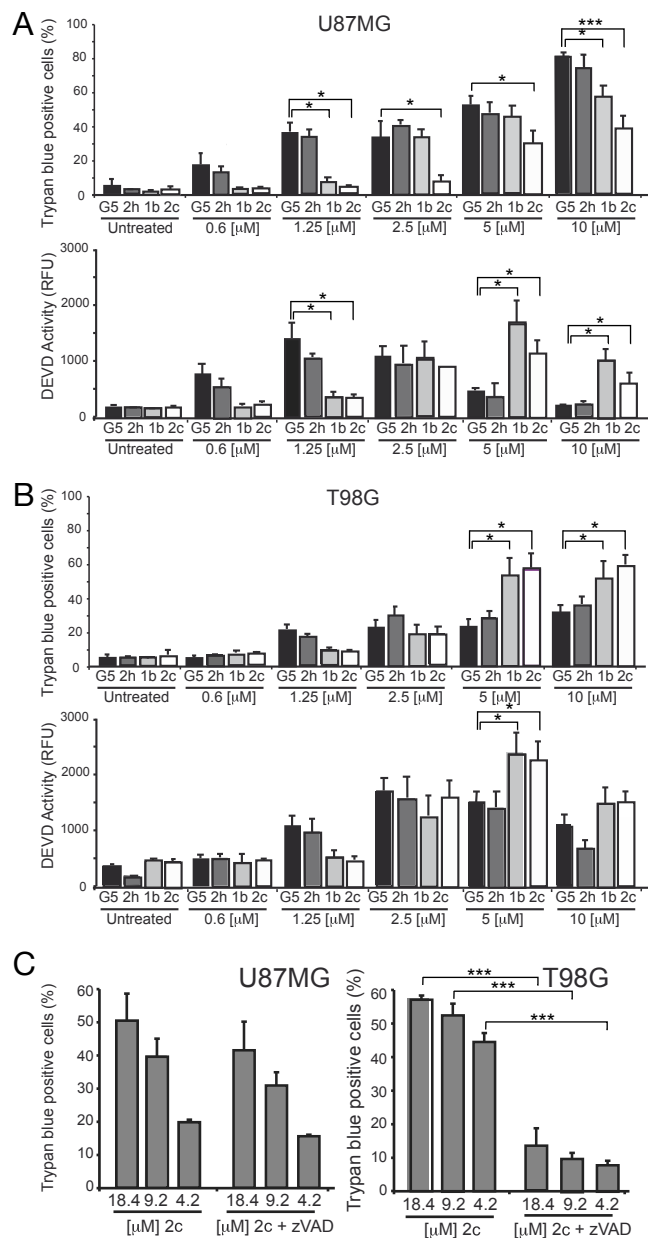


**Figure 3.** Apoptotic and necrotic responses induced by different dienones in U87MG (A) and T98G (B) cells. Cells were treated with the indicated concentrations of the different compounds for 24 hours. Upper: cell death as measured by percent of trypan blue-positive cells; lower: caspase activity measured with rhodamine 110 bis-(N-Z-L-aspartyl-L-glutamyl-L-valyl-aspartic acid amide) fluorogenic substrate (relative fluorescence units) (black, G5; grey, **2h**; light grey, **1b**; white, **2c**). (C): effect of caspase inhibitor zVAD-fmk on cell death induced by **2c** (percent of trypan blue-positive cells).

In summary, the simultaneous presence of the sulfone/sulfoxide and nitro groups in **2h** and G5 appears to promote a necrotic response; replacement of either group, as in **2c** and **1b**, lowers the necrotic activity of the N-SII and favors the induction of apoptosis.

The ability of the compound **2c** to kill preferentially through apoptosis suggests that it could represent a better choice for *in vivo* applications, with respect to G5. Moreover, compound **2c**, possessing a reactive OH group, appears to be a good compromise between cytotoxicity and the possibility to introduce modifications on the core to improve the inhibitor's drug-like properties. For these reasons **2c** was selected for further development.

**Deubiquitinase inhibition by G5 and 2c.** We evaluated the inhibitory profile of the two compounds against purified isopeptidases using ubiquitin-AMC as a substrate. Previous studies demonstrated that dienones are broad inhibitors, capable of inhibiting deubiquitinases but also deSUMOylase activities.<sup>35</sup> Thus, we investigated G5 and **2c** activities against ubiquitin carboxy-terminal hydrolases UCHL1, UCHL5 and the ubiquitin-specific protease USP2.

UCHL5/UCH37 is a proteasome-associated UCH, which, in conjunction with POH1/PSMD14 and USP14 provides to the proteasome the deubiquitinase activity.<sup>3</sup> Unlike UCHL1 and UCHL3, UCHL5 can also process poly-ubiquitin chains and previous studies identified UCHL5 as a target of dienone-based N-SIIs<sup>16</sup>.

Both G5 and **2c** weakly inhibit UCHL1 (Figure 4A) but are much less effective than other small-molecule inhibitors.<sup>36</sup> Conversely, both compounds exhibit a more pronounced inhibitory activity against UCHL5. G5 is considerably more potent than **2c**, as shown by the IC<sub>50</sub> values of 13.58 μM and 42.99 μM, respectively. Thus, UCHL5 inhibition may play an important role in eliciting the accumulation of poly-ubiquitinated proteins in cells treated with these compounds.

When USP2 activity was analyzed, again G5 showed some inhibitory activity (IC<sub>50</sub> 32.56 μM) whereas **2c** was almost inactive. This IC<sub>50</sub> value is in agreement with previous studies where a compound related to G5 was used.<sup>14,35</sup>

Finally, we also tested G5 and **2c** inhibitory potency against the isopeptidase USP18, which processes the Ub-like ISG15 protein and is a key regulator of the interferon response.<sup>37</sup> Both compounds inhibit USP18 activity, and **2c** appears to be slightly more active than G5, with IC<sub>50</sub> 21.20 μM and 33.23 μM, respectively. The ability of **2c** to inhibit USP18 was verified also in cells by co-expressing USP18 and a fusion between ISG15 and GFP.<sup>38</sup> When ISG15-GFP was co-expressed with USP18, accumulation of free GFP is predominant (Figure 4B). By contrast, in the presence of increasing concentrations of G5 or **2c**, accumulation of the uncleaved ISG15-GFP chimera can be appreciated. In the same assay, bortezomib failed in influencing USP18-dependent cleavage of ISG15-GFP.

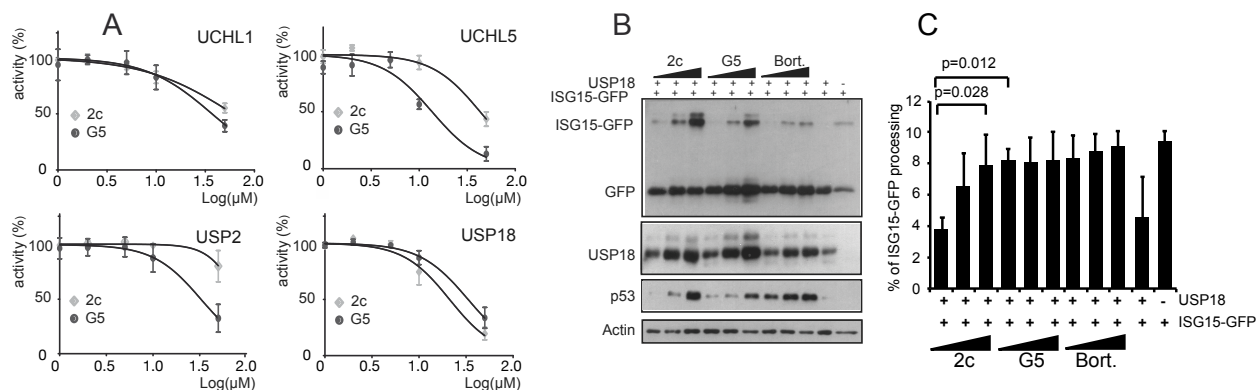


**Figure 4.** (A) Inhibition of ubiquitin-specific hydrolases UCHL1, UCHL5, USP2 and USP18 by G5 and **2c**. (B) Immunoblot analysis showing inhibition of USP18 in A549 cells co-expressing USP18 and the ISG15-GFP chimera; p53 levels were used to monitor the inhibition of the UPS. Inhibitor concentrations were: **2c** (2.5, 5, 10 μM); **G5** (1, 2.5, 5 μM); bortezomib (25, 50, 100 nM). Cellular lysates were generated after 24h of treatment. Under these concentrations comparable % of death in A549 lung cancer cells can be observed 48h later. (C) Quantitative densitometric analysis of immunoblots. Data are presented as the mean of two experiments.

**Analysis of 2c pro-apoptotic activity.** Next, to evaluate whether **2c** shows a strong and broad-spectrum of anti-proliferative activities, we calculated its IC<sub>50</sub> against several other cancer cell lines. Data in Table 3 indicate that **2c** anti-proliferative activity is indeed wide and mainly in the low μM range, as already observed for U87MG and T98G cell lines.

**Table 3.** Anti-proliferative activity of **2c** and PEGylated derivative **2cPC (11)** in different cell lines

Cell line		IC <sub>50</sub> (μM) <sup>a</sup>	
		<b>2c</b>	<b>11</b>
U87MG	glioblastoma	4.62	6.9
A375	melanoma	6.1	5.7
A549	lung cancer	16	22
HT29	colorectal adenocarcinoma	7.6	>100
Hep3B	hepatocellular carcinoma	8.5	
Mia PaCa-2	pancreatic cancer	35.2	

<sup>a</sup> From cell viabilities measured with a resazurin assay, 48 hours after treatments.

We then evaluated in more detail the effect of **2c** on the lung cancer cell line A549 that was later chosen for *in vivo* experimentation (vide infra). Initially, we compared the apoptotic response elicited by **2c**, G5 and bortezomib to identify the concentration ranges of the three inhibitors that induce comparable extents of cell death (Figure 5A). We then used these concentrations to compare the effects of the three inhibitors on the activity of the UPS and on the accumulation of the BH3-only protein Noxa, a sensor of endoplasmic reticulum stress and key element of the death pathway elicited by UPS inhibitors.<sup>14</sup> Immunoblot analysis (Figure 5B) demonstrated that at the lower concentrations bortezomib is more effective in eliciting accumulation of poly-ubiquitinated proteins and in stabilizing p53 with respect to **2c** or G5. Interestingly, when cell death is induced with similar intensity accumulation of Noxa is comparable in bortezomib and **2c** treatments, thus suggesting that ER stress is similarly evoked by the two compounds. By contrast, high doses of G5 less efficiently promote Noxa up-regulation, consistent with the possible engagement of a necrotic response (Figure 5B).

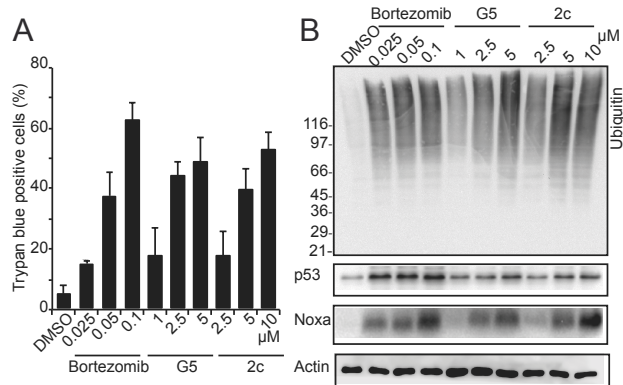
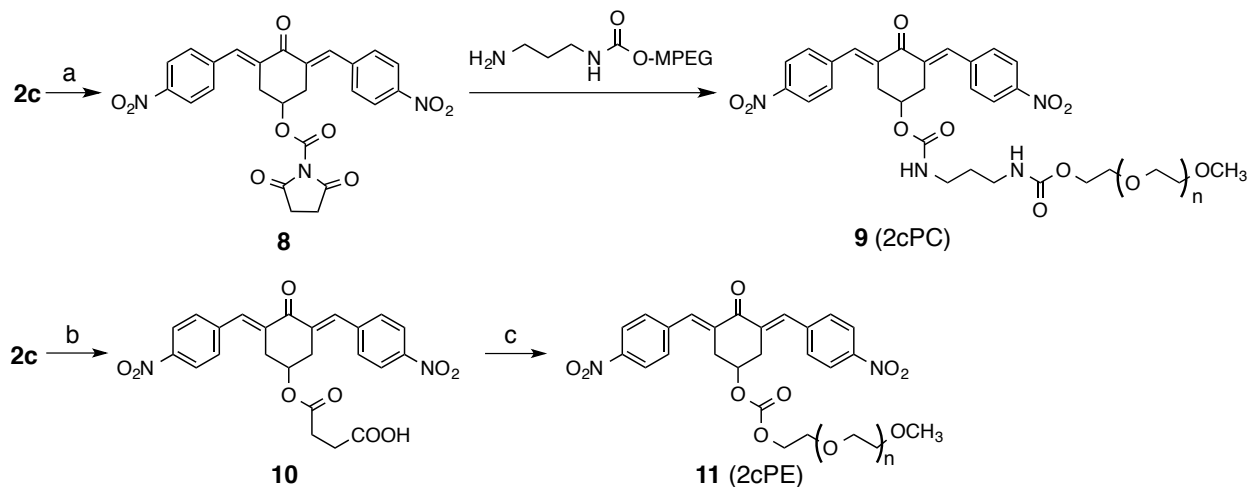


**Figure 5.** (A) Inhibitor concentrations eliciting comparable death percentage in A549 lung cancer cells, after 48 hours of treatment. (B) Immunoblot analysis of extracts from A549 cells treated as in A) and monitored for UPS inhibition, (poly-ubiquitin and p53 accumulation) and induction of ER-stress, (Noxa induction) after 24 hours of treatment.



**Synthesis and activity of a **2c** derivative optimized for in vivo studies.** **2c**, like many anticancer compounds, is poorly soluble in aqueous solutions. A common strategy for improving drugs solubility and bioavailability consists in the conjugation of the compound with polyethylene glycol (PEG). Despite the intrinsic limitation of a low drug/carrier mass ratio when used with low molecular weight drugs, polyethyleneglycol offers some advantages as a water soluble carrier for anticancer compounds.<sup>39-41</sup> We thus synthesized two soluble derivatives by conjugating **2c** to mono-methoxy PEG (5000 Da) via the OH group and suitable linkers (Scheme 3).

**Scheme 3.** PEGylation of **2c**.<sup>a</sup>



<sup>a</sup>Reagents and conditions: (a) *N,N'*-disuccinimidyl carbonate (75%); (b) succinic anhydride, DMAP (82%); (c) MPEG-OH, EDC, HOBT, TEA (70%).

For the synthesis of the first conjugate (**9**), with a dicarbamate linker (2cPC, 2c-PEG-Carbamate), **2c** was converted into the mixed carbonate **8** and then coupled with mono-PEGylated 1,3-diaminopropane (41 % overall yield). When tested on the panel of cancer cell lines, however, this conjugate was inactive, incapable of triggering cell death and reducing cell proliferation (data not shown). We thus synthesized a second derivative (**11**), in 57 % overall yield, by conjugating **2c** with PEG through a succinate linker (Scheme 3). We reasoned that this conjugate (2cPE, 2c-PEG-Ester), containing a more reactive diester linker, could act as a pro-drug, releasing the active species **2c** upon the action of cellular hydrolases<sup>42</sup> and, indeed, we found that **11** was active on three of the four cell lines tested (Table 3).

In melanoma A375 and glioblastoma U87MG cells the anti-proliferative activity of 2cPE (**11**) is identical to that of the parent molecule **2c** (Table 3). By contrast, in A549 and, even more so, in HT29, respectively lung and colon cancer derived cell lines, the PEGylated molecule is less effective in suppressing proliferation. To verify this observation, we compared the response of A549 cells to 2cPE (**11**) and **2c**, by scoring cell death with trypan-blue assay. Dose dependent studies (Figure 6A) and time course analysis (Figure 6C) confirm that 2cPE is less effective than **2c** in triggering cell death in A549 cells. An observation further corroborated by the analysis of poly-ubiquitin accumulation, p53 stabilization and Noxa induction (Supplementary Figure S2). Similar results were obtained in HT29 cells (Supplementary Figure S3).

On the opposite, in A375 cells, which show similar sensitivity to **2c** and 2cPE in resazurin assay (Table 3), cell death (Figure 6B), accumulation of poly-ubiquitinated proteins, p53 stabilization and Noxa up-regulation (Supplementary Figure S2) confirm that 2cPE behaves like the active compound **2c**. In summary, in A375 cells **2c** and the PEGylated derivative 2cPE are undistinguishable as UPS inhibitors and inducers of cell death, while A549 and HT29 cells show some resistance to the PEGylated derivative 2cPE (**11**).

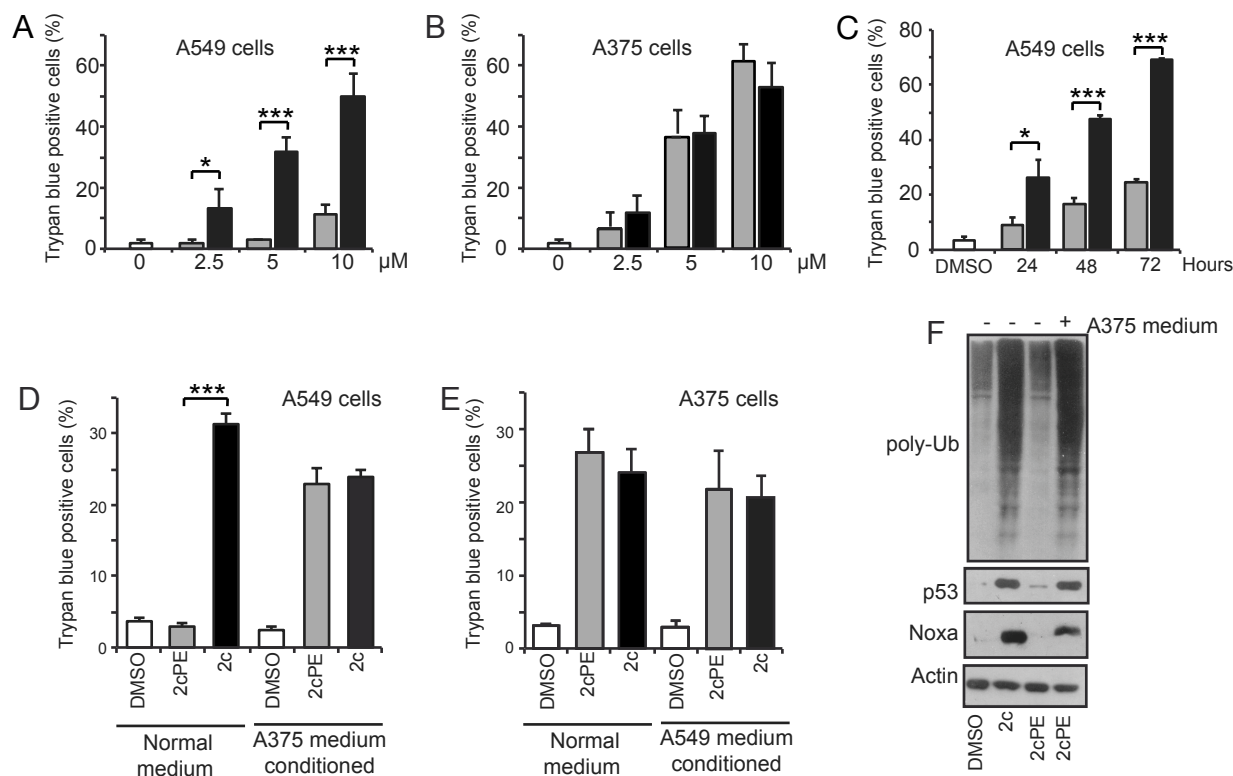


**Figure 6.** Cell death, after 48 hours, as a function of concentration in A549 (A) and A375 (B) cells treated with 2.5-10 μM **2c** (black bars) and **2cPE** (**11**) (grey bars). (C) Cell death as a function of time in A549 cells treated with 10 μM **2c** (black bars) and **11** (grey bars) for 24-72 hours. (D) Response to 10 μM **2c** and **2cPE** (**11**) of A549 cells grown in normal and A375 conditioned medium. (E) Response to 10 μM **2c** and **2cPE** (**11**) of A375 cells grown in normal and A549 conditioned medium. (F) Immunoblot analysis showing poly-ubiquitin accumulation, p53 stabilization and Noxa induction in A549 cells treated with 10 μM **2c** (second lane) and **2cPE** (**11**) in normal and A375 conditioned medium (third and fourth lane, respectively). DMSO is the negative control throughout.

**Activation of the 2cPE pro-drug by secreted esterases.** A different pattern of expression of enzymes capable to hydrolytically release the active species **2c** from the PEG conjugate might explain the differential responsiveness of the four cell lines to **2cPE** (Table 3). This hypothesis is supported by the observation that unresponsive A549 cells become fully responsive to **2cPE** when they are grown in the presence of A375 conditioned medium (Figure 6D), while A375 cells retain their responsiveness to **2cPE** also in the presence of A549 conditioned medium (Figure 6E). Similar results were obtained with HT29 cells (Supplementary Figure S3). Accumulation of poly-ubiquitin chains, stabilization of p53 and Noxa induction (Figure 6F) confirm that, in the presence of conditioned medium from A375 cells, the activities of **2c** and **2cPE** are indistinguishable, thus indicating that the prodrug is readily converted into the active molecule by this medium.

These results indicate that the response to **2cPE** (Table 3) of different cell lines depends on their ability to secrete an esterase activity capable of releasing **2c** from the pro-drug. To gain insight into the enzymes that might be responsible for such processing we applied a bioinformatics analysis.

Initially, the different esterases encoded by the human genome were extracted using GEO categories and HomoloGene.<sup>43</sup> In this manner we generated a list of 173 putative esterases. Next, to understand which secreted esterase exhibited an expression profile compatible with the responsiveness to **2cPE**, we interrogated gene expression profiles available for A375, A549 and HT29 cells<sup>44</sup> with our list. The expression of the candidate esterase is expected to be high in A375, reduced in A549 cells and even more reduced in HT29 cells. Seven esterases satisfied this expression profile, as illustrated in figure 7A. Among these potential candidates, we have focused our attention on the Phospholipase A2 group 7 (encoded by the PLA2G7 gene). This enzyme, also known as PAF-AH (platelet activating factor acetylhydrolase), has been extensively characterized,<sup>45</sup> and the crystal structures of both the ligand-free and of the paraoxon covalently-inhibited enzyme are reported.<sup>46</sup> PLA2G7, which hydrolyses the ester

bond at the sn-2 position of phospholipid substrates shows a canonical  $\alpha/\beta$  hydrolase fold, and it has an interface binding area that makes it capable of binding to the hydrophobic portions of lipoproteins, or to the internal hydrophobic region of cell membranes. The interface is located at the end of a long hydrophobic channel that leads to the catalytic serine and to the oxyanion hole. Polyethylene glycol is known to activate the phospholipase activity of the enzyme, probably by stabilizing the interface complex between the lipase and the hydrophobic inner regions of cell membranes.<sup>47</sup> To verify that PLA2G7 can accept 2cPE as a substrate, we have built a model of the tetrahedral covalent intermediate for the hydrolysis of **2c** conjugated to an ethylene glycol dodecamer through the same succinate linker present in 2cPE. The crystal structure of the paraoxon covalently inhibited enzyme was used as a starting point and stepwise mutated and optimized to build the model. The unique conformation corresponding to a stable and productive intermediate according to the stereoelectronic theory of Deslongchamps<sup>48,49</sup> is reported in Figure 7B. In this conformation, the first five units of the PEG chain lie inside the hydrophobic channel of the enzyme, and **2c** is partially buried inside the catalytic site, which appears to be broad and flexible enough to host this rather large structure. The two nitro groups have a key role in stabilizing this intermediate: one of them is found at hydrogen bond distance with the hydroxy groups of serines 319 and 349, while the aromatic ring establishes  $\pi$ -stacking interactions with phenylalanine 322 and further hydrophobic contacts with histidine 351 (omitted for clarity in the figure). The other nitro group is in contact with the side chain of arginine 218. Interactions of arginine and serine with the nitro groups of a ligand, such as those found in this model, are well known in antibodies and receptor complexes.<sup>50</sup>

The model confirms that 2cPE could be a substrate for phospholipase A2 secreted by A375 cells and thus supports the hypothesis that lack of this enzyme, or of other esterases that can activate the pro-drug, might explain the different low response of A549 and HT29 cell lines (Table 3). To prove the involvement of PLA2G7 in pro-drug maturation, we generated by retroviral infection, A549 cells expressing PLA2G7 isolated from A375 cells. As control we used A549 cells expressing only the resistance gene PURO. In the presence of PLA2G7, A549 cells dramatically increase responsiveness to the pro-drug in terms of cell death (Fig. 7C). Further evidence was obtained by incubating **2cPE** with a commercially available preparation of PLA2G7; mass spectrometry analysis indicated that the enzyme was able to completely hydrolyse **2cPE** in phosphate buffer at 25° C for 8 hours, yielding **2c** and PEG5000 (see supporting information, page S7). Conversely, no hydrolysis was observed when **2cPE** was incubated in the buffer for the same time without the enzyme.

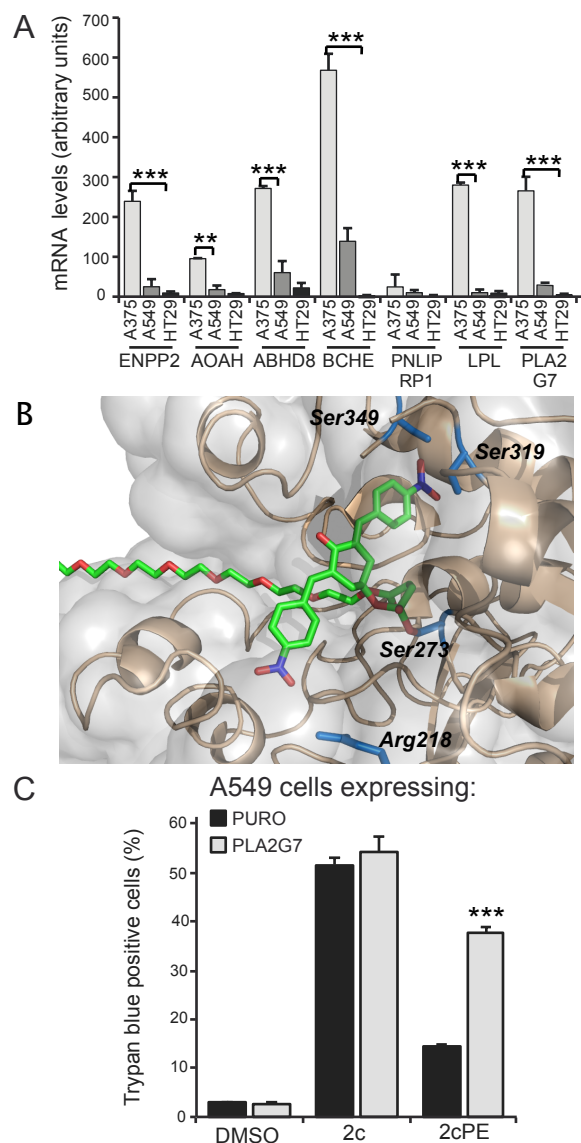


**Figure 7.** (A) Expression profiles in A375, A549 and HT29 cells of seven candidate esterases for the hydrolysis of 2cPE. (B) Optimized model of the rate determining tetrahedral intermediate for hydrolysis of 2cPE catalyzed by phospholipase A (PLA2G7). The model was built from the crystal structure of PLA2G7 covalently inhibited by paraoxon (PDB: 3D5E). (C) Response to 10  $\mu$ M **2c** and **2cPE** of A549 cells engineered to express PLA2G7 or the control gene PURO. Trypan blue analysis was performed 48 hours after treatment.

**2cPE inhibits tumor growth in mice.** With convincing evidence in hand that the pro-drug 2cPE (**11**) is converted into the active form **2c** by secreted hydrolases and PLA2G7 in particular, we set to analyzing whether the PEG conjugate displays anti-tumor activity *in vivo*. To this end we selected A549 lung cancer cells, even if these cells showed a low response to the pro-drug in culture. However, we expected that, in animals, the pro-drug should be efficiently processed by mouse secreted 2cPE activator PLA2G7 and, possibly, other secreted esterases.

Initially toxicity tests indicated that 2cPE is well tolerated with transient minimal effect on the animal's body weight up to 800 mg/kg. All treated groups showed slight (2%) body weight loss over the course of the first week, independently from the doses. Subsequently, the body weight of all animals steadily increased until the end of the

study with final 6 – 8% gain in body weight (Supplementary Figure S4). No gross toxicity was observed throughout the treatment and 2cPE did not induce any behavioral change or grossly visible pathological changes.

A549 lung carcinoma xenografts were generated in immune-compromised mice and when the tumors reached the size of 0.1 mm, 2cPE (170 mg/kg) was administered three times every 4 days. After one week from last injection (day 15) the percentage of tumor volume inhibition (*TGI*) was 72% and 78%, respectively for subcutaneous and intravenous treatments (Figure 8A). At the end of the experiment, the reduction of primary tumor growth was particularly marked (*TGI* 79%) in the i.v. treated group. No significant adverse effects were observed correlated to drug administration.

To further characterize the *in vivo* anti-tumor activity of 2cPE we evaluated the cellular responses in normal mouse tissues (liver, kidney and spleen) and in the tumor. Immunoblot analysis of tissue extracts confirms also *in vivo* the up-regulation of p53 and Noxa following 2cPE treatment (Figure 8B). This up-regulation was much more evident in the tumor compared to normal tissue. To exclude species-specific enrichment of the antibody against p53, we used, in addition to DO-1 antibody, the 421 antibody, which recognizes with similar affinity the human and murine proteins.

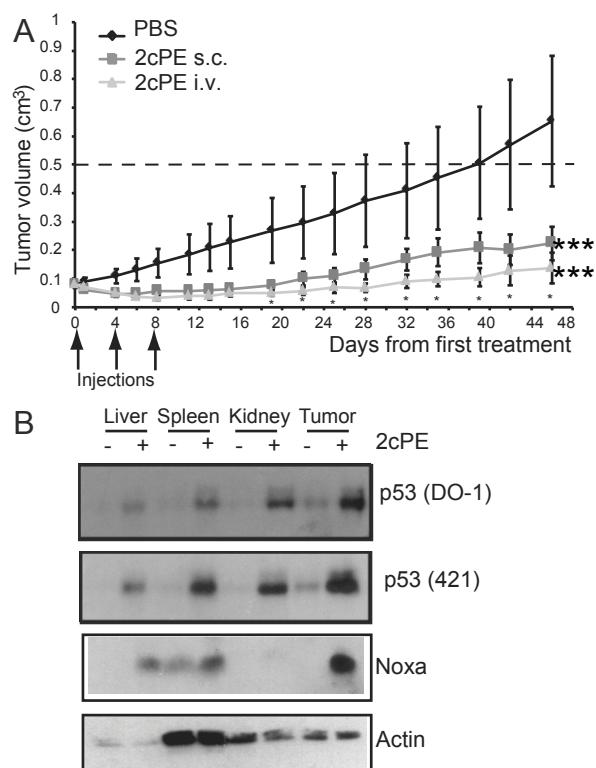


**Figure 8.** (A) Variations of A549 lung carcinoma xenografts volume in mice following subcutaneous (s.c.) and intravenous (i.v.) treatments with 2cPE (170 mg/kg). (B) Immunoblot analysis showing up-regulation of p53 and Noxa proteins in tissues of mice treated with 2cPE. Mice in which the tumor mass reached the size of at least 0.5 cm<sup>3</sup> were treated for the first time with 170mg/kg of 2cPE and 48 hours later they were sacrificed for the generation of tissue extracts. p53 was detected with DO-1 and 421 antibodies, showing no significant difference.

## CONCLUSIONS

Several studies have established that compounds characterized by the presence of the 1,5-diaryl-3-oxo-1,4-pentadienyl pharmacophore exhibit cytotoxic activities *in vitro* against multiple cancer cell lines.<sup>29</sup> While different cellular thiols may in principle react with these Michael acceptors, isopeptidases, a heterogeneous family of cysteine-proteases, are important targets for their anti-neoplastic activity. These inhibitors, also called N-SIIs, can trigger both necrosis and apoptosis, depending on the cellular context.<sup>24,33,34</sup> In this work we have shown that the cytotoxicity of a family of dienones structurally related to sulfone **G5** is directly correlated with the electrophilicity of the dienone system. This provides indirect evidence that the biological activity of these compounds is due to their ability to act as mechanism-based inhibitors of cysteine proteases. We have also demonstrated that by varying the substituents on the aromatic rings and the structure of the cyclic scaffold it is possible to limit necrosis and to favor cell death by apoptosis. This has led to the identification of compound **2c**, based on a 4-hydroxycyclohexanone scaffold, as a good candidate for further development.

Analysis of the inhibitor activities has evidenced that **G5** is in general a more potent inhibitor of DUBs such as UCHL1, UCHL5 and USP2 compared to **2c**. By contrast, **2c** functions, to some extent, as a better inhibitor for the deISGylase USP18. In this scenario the dichotomy apoptosis/necrosis might reflect different patterns of cysteine-protease inhibition. Certainly, in view of the existence of additional cellular targets, alternative hypothesis are possible and further studies will be necessary to clarify this point.

It has been suggested that similar N-SIIs, although characterized by a broad spectrum of activity, can nevertheless exhibit preference for certain targets.<sup>15-17,35</sup> In this view, the lower IC<sub>50</sub> for proteasome-associated deubiquitinase UCHL5 compared to other USPs, displayed by both **G5** and **2c**, can explain their action as UPS inhibitors,<sup>13,14,16</sup> even if additional mechanisms must also be taken into account.<sup>23</sup>

In this study we have also designed and synthesized the first N-SII pro-drug (**2cPE**), by conjugating compound **2c** with PEG, through a cleavable diester linker. This strategy has overcome the solubility issue and has provided effective anti-tumoral activity *in vivo*, after administration of the pro-drug by intravenous injections. From the diverse response *in vitro* of different cell lines to the pro-drug, and by applying bioinformatics analysis and structural studies, we have identified in PLA2G7/PAF-AH a key esterase involved in pro-drug maturation. This esterase has been proposed as an activating factor for anticancer pro-drugs and delivery systems due to its overexpression in breast, stomach, colorectal, pancreatic, prostate and liver cancers. Anticancer lipids have been included in liposomes to be hydrolysed by phospholipase A2,<sup>51</sup> and designed phospholipids containing PEG350 or PEG2000 chains linked to phosphatidylethanolamine by a carbamate linkage have proven to be substrates for the enzyme.<sup>52</sup> PLA2G7 is primarily produced by macrophages and circulates in plasma in active form as a complex with LDL and HDL.<sup>53</sup> This pattern of expression explains why A549 cells, which are unresponsive to **2cPE** *in vitro*, become fully responsive when evaluated *in vivo*.

The antineoplastic activity of **2cPE** *in vivo* was accompanied by the up-regulation of p53 and of the pro-apoptotic protein Noxa. This up-regulation was more marked in tumor cells compared to liver, spleen and kidney. Importantly, although pro-apoptotic genes were up-regulated also in normal tissues at some extents, the animals did not show any effect of toxicity. Both the reduced up-regulation of the apoptotic program, in normal cells and their higher intrinsic resistance to stress, can explain the absence of evident toxicity.

In summary, isopeptidase inhibitors represent interesting tools in anti-neoplastic therapy. Understanding mechanisms of actions, improving the delivery, for instance by the generation of pro-drugs through a cleavable PEGylation as described here for the first time, and further medicinal chemistry approaches to improve activity are efforts that need pursuing to provide additional anti-cancer therapeutics.

## EXPERIMENTAL SECTION

All biologically evaluated compounds had a purity > 95% as determined by HPLC analyses (see supporting information).

**Chemistry: general protocols.** Melting points are uncorrected and are given in Celsius degrees. <sup>1</sup>H NMR and <sup>13</sup>C NMR spectra were recorded in CDCl<sub>3</sub>, unless otherwise stated, on Jeol EX400 (400 MHz) and Varian X500 (500 MHz) spectrometers; chemical shifts are given in ppm relative to tetramethylsilane. IR spectra were obtained as Nujol mulls with a Thermo-Nicolet AVATAR 320 FT-instrument. Electron impact mass spectra (MS) were obtained on a Varian Saturn 2200 spectrometer equipped with a direct insertion probe. Electrospray mass spectra (ESI-MS) were obtained with a Bruker Daltonics Esquire 4000 spectrometer. Flash chromatography was performed on silica gel 60 (Merck, 230–400 mesh). 4*H*-Thiopyran-4-one-1,1-dioxide,<sup>25</sup> and compounds **1a**,<sup>26</sup> **2a**,<sup>27</sup> **2b**,<sup>27</sup> **2e**<sup>30</sup> were synthesized according to the literature. Poly(ethylene glycol) methyl ether (Sigma-Aldrich) and all the

PEGylated derivatives were co-evaporated twice with dry dichloromethane and dried under vacuum immediately prior to use.

**(3Z)-3-[(4-nitrophenyl)methylene]-4H-tetrahydrothiopyran-4-one (5).** A suspension of tetrahydrothiopyran-4-one (23.2 g, 0.2 mol) and 4-nitrobenzaldehyde (15.1 g, 0.1 mol) in 100 mL water containing MgSO<sub>4</sub>·7H<sub>2</sub>O (14.8 g, 0.06 mol) and NaOH (5 g, 0.125 mol) was stirred at room temperature for 20h. The solid was collected, dried and washed repeatedly with diethyl ether to remove the excess tetrahydrothiopyran-4-one. The product, containing approximately equal amounts of the aldol diastereoisomers, was dehydrated for 1h in refluxing ethanol (100 mL) containing conc. HCl (10 mL). The mixture was cooled to 25 °C and filtered, giving the crude enone **5** (13.9 g, 56%); m.p. 105–106 °C (from ethanol). <sup>1</sup>H NMR: δ = 2.05 (t, 2H), 2.96 (t, 2H), 3.76 (s, 2H), 7.48 (s, 1H), 7.51 (d, 2H), 8.27 ppm (d, 2H). <sup>13</sup>C NMR: δ = 26.0, 28.5, 41.5, 123.8, 130.3, 132.4, 137.2, 141.3, 147.6, 198.5 ppm. IR: ν = 1672 (C=O), 1515 and 1344 cm<sup>-1</sup> (NO<sub>2</sub>). MS: *m/z* 249 (M<sup>+</sup> 45%), 232 (100%). Elemental analysis calculated (%) for C<sub>12</sub>H<sub>11</sub>NO<sub>3</sub>S: C 57.8, H 4.45, N 5.62. Found: C 57.8, H 4.34, N 5.30.

**General procedure for the synthesis of dienones 1, 2 and 6 by the acid-catalyzed Knoevenagel condensation.** A solution, or mixture, of the appropriate aryl aldehyde (0.1 mol) and cyclic ketone (0.05 mol) in 30 mL ethanol containing 3mL of 37% HCl was heated at gentle reflux for 1-2 h.<sup>26</sup> Alternatively, the reaction mixture, in a stoppered vial, was heated at 120 °C for 20 min in a microwave reactor. The solution was cooled in an ice bath, the product was collected by filtration, washed with ethanol and dried.

**(3Z,5Z)-3,5-Bis[(4-nitrophenyl)methylene]-tetrahydro-4H-thiopyran-4-one-1,1-dioxide (G5).** 45% from tetrahydro-4H-thiopyran-4-one-1,1-dioxide and 4-nitrobenzaldehyde; m.p. 226–230 °C (lit.<sup>54</sup> 233.5–234.5 °C). <sup>1</sup>H NMR ([d.]DMSO): δ = 4.70 (s, 4H, CH<sub>2</sub>), 7.70 (d, 4H, ArH), 7.95 (s, 2H, =CH) 8.3 ppm (d, 4H, ArH). <sup>13</sup>C NMR ([d.]DMSO): δ = 52.5, 123.8, 131.8, 130.7, 139.9, 140.8, 147.6, 184.4 ppm. IR: ν = 1677 (C=O), 1513 and 1350 (NO<sub>2</sub>), 1320 and 1136 cm<sup>-1</sup> (SO<sub>2</sub>). MS: *m/z* 414 (M<sup>+</sup> 5%), 333 (100%).

**(3Z,5Z)-3,5-Bis[(4-methoxyphenyl)methylene]-tetrahydro-4H-thiopyran-4-one-1,1-dioxide (1b).** 69% from tetrahydro-4H-thiopyran-4-one-1,1-dioxide and p-tolualdehyde; m.p. 186–188 °C. <sup>1</sup>H NMR: δ = 2.40 (s, 6H), 4.46 (s, 4H), 7.25 (d, 4H), 7.31 (d, 4H), 7.98 ppm (s, 2H). <sup>13</sup>C NMR: δ = 21.6, 53.2, 129.8, 129.9, 125.9, 130.8, 140.7, 144.3, 186.1 ppm. IR: ν = 1664 (C=O), 1333 and 1127 cm<sup>-1</sup> (SO<sub>2</sub>). MS: *m/z* 352 (M<sup>+</sup> 20%), 273 (100%).

**(3Z,5Z)-3,5-Bis[(4-hydroxyphenyl)methylene]-tetrahydro-4H-thiopyran-4-one-1,1-dioxide (1c).** 23% from tetrahydro-4H-thiopyran-4-one-1,1-dioxide and 4-hydroxybenzaldehyde; m.p. 244–246 °C. <sup>1</sup>H NMR ((CD<sub>3</sub>)<sub>2</sub>CO): δ = 3.0 (s, 2H), 4.57 (s, 4H), 6.94 (d, 4H), 7.41 (d, 4H), 7.87 ppm (s, 2H). <sup>13</sup>C NMR ((CD<sub>3</sub>)<sub>2</sub>CO): δ = 52.8, 116.1, 132.6, 125.6, 125.8, 142.3, 159.5, 184.2 ppm. IR: ν = 3388 (OH), 1659 (C=O), 1304 and 1128 cm<sup>-1</sup> (SO<sub>2</sub>). MS: *m/z* 356 ([M-2H]<sup>+</sup> 58%).

**(3Z,5Z)-3,5-Bis[(4-methoxyphenyl)methylene]-tetrahydro-4H-thiopyran-4-one-1,1-dioxide (1d).** 50% from tetrahydro-4H-thiopyran-4-one-1,1-dioxide and p-anisaldehyde; m.p. 175–177 °C. <sup>1</sup>H NMR: δ = 3.83 (s, 6H), 4.46 (s, 4H), 6.96 (d, 4H), 7.40 (d, 4H), 7.97 ppm (s, 2H). <sup>13</sup>C NMR: δ = 53.3, 55.5, 114.6, 131.9, 124.6, 126.2, 143.9, 161.2, 185.8 ppm. IR: ν = 1659 (C=O), 1318 and 1125 cm<sup>-1</sup> (SO<sub>2</sub>). MS: *m/z* 384 (M<sup>+</sup> 75%), 88 (100%).

**(3Z,5Z)-3,5-Bis[(4-phenoxyphenyl)methylene]-tetrahydro-4H-thiopyran-4-one-1,1-dioxide (1e).** 50% from tetrahydro-4H-thiopyran-4-one-1,1-dioxide and 4-phenoxybenzaldehyde; m.p. 165–168 °C. <sup>1</sup>H NMR: δ = 4.40 (s, 4H), 7.00-7.08 (m, 8H), 7.17 (t, 2H), 7.35-7.41 (m, 8H), 7.96 ppm (s, 2H). <sup>13</sup>C NMR: δ = 53.2, 118.3, 120.0, 124.5, 125.5, 130.1, 131.8, 128.0, 143.6, 155.8, 159.5, 186.0 ppm. IR: ν = 1666 (C=O), 1308 and 1133 cm<sup>-1</sup> (SO<sub>2</sub>). MS: *m/z* 443 ([M-SO<sub>2</sub>]<sup>+</sup> 100%).

**(3Z,5Z)-3,5-Bis[(4-cyanophenyl)methylene]-tetrahydro-4H-thiopyran-4-one-1,1-dioxide (1g).** 20% from tetrahydro-4H-thiopyran-4-one-1,1-dioxide and 4-cyanobenzaldehyde; m.p. 260–262 °C. <sup>1</sup>H NMR ([d.]DMSO): δ = 4.69 (s, 4H), 7.93 (s, 2H), 7.72 (d, 4H), 8.00 ppm (d, 4H). <sup>13</sup>C NMR ([d.]DMSO): δ = 52.1, 111.9, 118.6, 130.2, 140.0, 130.7, 132.6, 138.1, 184.6 ppm. IR: ν = 2232 (CN), 1692 (C=O), 1327 and 1123 cm<sup>-1</sup> (SO<sub>2</sub>). MS: *m/z* 374 (M<sup>+</sup> 30%), 309 (100%). Elemental analysis calculated (%) for C<sub>21</sub>H<sub>14</sub>N<sub>2</sub>O<sub>3</sub>S: C 67.4, H 3.77, N 7.48. Found: C 67.0, H 3.81, N, 7.37.

**(3Z,5Z)-3,5-Bis[(3-nitro-4-methoxyphenyl)methylene]-tetrahydro-4H-thiopyran-4-one-1,1-dioxide (1h).** 54% from tetrahydro-4H-thiopyran-4-one-1,1-dioxide and 3-nitro-4-methoxybenzaldehyde; m.p. 259–260 °C. <sup>1</sup>H NMR ([D<sub>6</sub>]DMSO): δ = 4.00 (s, 6H), 4.74 (s, 4H), 7.45 (s, 2H), 7.85 (s, 2H), 7.88 (d, 2H), 8.09 ppm (d, 2H). <sup>13</sup>C NMR ([d.]DMSO): δ = 51.9, 57.0, 114.7, 126.6, 136.4, 125.9, 128.1, 139.5, 152.7, 184.2 ppm. IR: ν = 1696 (C=O), 1531 and 1340 (NO<sub>2</sub>), 1311 and 1131 cm<sup>-1</sup> (SO<sub>2</sub>). MS: *m/z* 474 (M<sup>+</sup> 1%), 393 (100%). Elemental analysis calculated (%) for C<sub>21</sub>H<sub>18</sub>N<sub>2</sub>O<sub>9</sub>S: C 53.16, H 3.82, N 5.90. Found: C 52.77, H 3.80, N 5.54.

**(3*Z*,5*Z*)-3,5-Bis[(3-nitrophenyl)methylene]-tetrahydro-4*H*-thiopyran-4-one-1,1-dioxide (1i).** 21% from tetrahydro-4*H*-thiopyran-4-one-1,1-dioxide and 3-nitrobenzaldehyde; m.p. 230–231 °C. <sup>1</sup>H NMR ([d.]DMSO): δ = 4.78 (s, 4H), 7.78 (t, 2H), 7.97 (s, 2H), 7.99 (s, 2H), 8.29 (d, 2H), 8.34 ppm (d, 2H). <sup>13</sup>C NMR ([d.]DMSO): δ = 52.5, 124.7, 125.1, 130.6, 130.9, 135.6, 136.7, 140.3, 148.6, 185.5 ppm. IR: ν = 1690 (C=O), 1530 and 1350 (NO<sub>2</sub>), 1320 and 1123 cm<sup>-1</sup> (SO<sub>2</sub>). MS: *m/z* 414 (M<sup>+</sup> 10%), 333 (100%). Elemental analysis calculated (%) for C<sub>19</sub>H<sub>14</sub>N<sub>2</sub>O<sub>7</sub>S: C 55.1, H 3.41, N 6.76, S 7.74. Found: C 54.7, H 3.38, N 6.44, S 7.55.

**(2*E*,6*E*)-2,6-Bis[(4-nitrophenyl)methylene]-4-hydroxycyclohexanone (2c).** 78% from 4-hydroxycyclohexanone and 4-nitrobenzaldehyde; m.p. 210–213 °C. <sup>1</sup>H NMR ([d.]DMSO): δ = 2.98 (dd, 2H), 3.09 (dd, 2H), 4.07-4.13 (m, 1H), 5.04 (d, 1H), 7.7 (s, 2H), 7.8 (d, 4H), 8.3 ppm (d, 4H). <sup>13</sup>C NMR ([d.]DMSO): δ = 36.0, 63.0, 123.8, 131.4, 134.0, 137.1, 142.2, 147.2, 188.9 ppm. IR: ν = 3539 (OH), 1668 (C=O), 1508 and 1342 cm<sup>-1</sup> (NO<sub>2</sub>). ESI-MS: *m/z* 403 (MNa<sup>+</sup>), 381 (MH<sup>+</sup>). Elemental analysis calculated (%) for C<sub>20</sub>H<sub>16</sub>N<sub>2</sub>O<sub>6</sub>: C 63.2, H 4.24, N 7.37. Found: C 62.9, H 4.19, N 7.32.

**Ethyl (3*E*,5*E*)-3,5-bis[(4-nitrophenyl)methylene]-4-oxocyclohexanecarboxylate (2d).** 36% from ethyl 4-oxocyclohexanecarboxylate and 4-nitrobenzaldehyde; m.p. 172–174 °C. <sup>1</sup>H NMR: δ = 1.16 (t, 3H), 2.76-2.84 (m, 1H), 3.06-3.24 (m, 4H), 4.12 (q, 2H), 7.56 (d, 4H), 7.85 (s, 2H), 8.27 ppm (d, 4H). <sup>13</sup>C NMR: δ = 14.2, 30.5, 3961.4, 123.8, 130.9, 135.9, 136.4, 141.7, 147.5, 173.2, 187.7 ppm. IR: ν = 1723 (C=O), 1673 (C=O), 1512 and 1340 cm<sup>-1</sup> (NO<sub>2</sub>). MS: *m/z* 436 (M<sup>+</sup> 50%), 419 (100%).

**(3*E*,5*E*)-Tetrahydro-3,5-bis[(4-nitrophenyl)methylene]-4*H*-pyran-4-one (2f).** 24% from tetrahydro-4*H*-pyran-4-one and 4-nitrobenzaldehyde; m.p. 263–265 °C (lit.<sup>54</sup> 272–273 °C). <sup>1</sup>H NMR ([d.]DMSO): δ = 4.96 (s, 4H), 7.73 (d, 4H), 7.77 (s, 2H), 8.28 ppm (d, 4H). <sup>13</sup>C NMR ([d.]DMSO): δ = 68.2, 124.2, 132.1, 133.5, 136.8, 140.9, 148.0 ppm. IR: ν = 1682 (C=O), 1514 and 1347 cm<sup>-1</sup> (NO<sub>2</sub>). MS: *m/z* 366 (M<sup>+</sup> 10%), 349 (100%).

**(3*Z*,5*Z*)-Tetrahydro-3,5-bis[(4-nitrophenyl)methylene]-4*H*-thiopyran-4-one (2g).** 41% from tetrahydro-4*H*-thiopyran-4-one and 4-nitrobenzaldehyde; m.p. 220–223 °C (lit.<sup>54</sup> 224–225 °C). <sup>1</sup>H NMR: δ = 3.87 (s, 4H), 7.55 (d, 4H), 7.77 (s, 2H), 8.29 ppm (d, 4H). <sup>13</sup>C NMR: δ = 30.1, 124.0, 130.6, 134.6, 136.2, 141.3, 147.7, 188.0 ppm. IR: ν = 1667 (C=O), 1509 and 1342 cm<sup>-1</sup> (NO<sub>2</sub>). MS: *m/z* 382 (M<sup>+</sup>, 20%).

**(3*Z*,5*Z*)-Tetrahydro-3,5-bis-[(4-fluorophenyl)methylene]-4*H*-tetrahydrothiapyran-4-one (3).** 54% from tetrahydro-4*H*-thiopyran-4-one and 4-fluorobenzaldehyde; m.p. 122–124 °C. <sup>1</sup>H NMR: δ = 3.88 (s, 4H), 7.11–7.38 (m, 4H), 7.73 ppm (s, 2H). <sup>13</sup>C NMR: δ = 30.0, 115.4 (d, *J*<sub>C-F</sub> = 22 Hz), 130.8 (d, *J*<sub>C-F</sub> = 3 Hz), 131.6 (d, *J*<sub>C-F</sub> = 8 Hz), 133.2 (d, *J*<sub>C-F</sub> = 1 Hz), 135.4, 162.5, (d, *J*<sub>C-F</sub> = 251 Hz), 188.4 ppm. IR: ν = 1662 (C=O), 1510 and 1330 cm<sup>-1</sup> (NO<sub>2</sub>). MS: *m/z* 328 (M<sup>+</sup> 100%). Elemental analysis calculated (%) for C<sub>19</sub>H<sub>14</sub>F<sub>2</sub>O<sub>5</sub>S: C 69.5, H 4.30. Found: C 69.3, H 4.41%.

**(3*Z*,5*Z*)-3-[(4-hydroxyphenyl)methylene]-5-[(4-nitrophenyl)methylene]-4*H*-tetrahydrothiapyran-4-one (6j).** 44% from **5** and p-hydroxybenzaldehyde; m.p. 178–180 °C. <sup>1</sup>H NMR ([d.]DMSO): δ = 3.93 (s, 2H), 3.98 (s, 2H), 6.85 (d, 2H), 7.42 (d, 2H), 7.56 (s, 1H), 7.61 (s, 1H), 7.73 (d, 2H), 8.25 (d, 2H), 10.0 ppm (broad, 1H). <sup>13</sup>C NMR ([d.]DMSO): δ = 29.0, 29.6, 115.7, 123.6, 125.4, 130.8, 131.2, 131.8, 132.8, 136.9, 137.3, , 141.6, 146.9, 158.9, 187.7 ppm. IR: ν = 3451 (OH), 1660 (C=O), 1519 and 1347 cm<sup>-1</sup> (NO<sub>2</sub>). MS: *m/z* 353 (M<sup>+</sup> 100%).

**(3*Z*,5*Z*)-3-[(4-methoxyphenyl)methylene]-5-[(4-nitrophenyl)methylene]-4*H*-tetrahydrothiapyran-4-one (6k).** 95% from **5** and p-methoxybenzaldehyde; m.p. 152–154 °C. <sup>1</sup>H NMR: δ = 3.74 (s, 2H), 3.84 (s, 3H), 3.96 (s, 2H), 6.96 (d, 2H), 7.39 (d, 2H), 7.51 (d, 2H), 7.73 (s, 1H), 7.77 (s, 1H), 8.27 ppm (d, 2H). <sup>13</sup>C NMR: δ = 29.9, 30.4, 55.5, 114.3, 123.9, 127.5, 130.6, 131.3, 132.4, 133.1, 136.9, 138.4, , 142.0, 147.5, 160.7, 188.4 ppm. IR: ν = 1653 (C=O), 1514 and 1344 (NO<sub>2</sub>). MS: *m/z* 367 (M<sup>+</sup> 100%). Elemental analysis calculated (%) for C<sub>20</sub>H<sub>17</sub>NO<sub>4</sub>S: C 65.38, H 4.66, N 3.81. Found: C 65.01, H 4.64, N 3.72.

**(3*Z*,5*Z*)-3-[(4-methylphenyl)methylene]-5-[(4-nitrophenyl)methylene]-4*H*-tetrahydrothiapyran-4-one (6l).** 73% from **5** and p-tolualdehyde; m.p. 139–142 °C. <sup>1</sup>H NMR ([d.]DMSO): δ = 2.32 (s, 3H), 3.95 (s, 2H), 3.98 (s, 2H), 7.26 (d, 2H), 7.42 (d, 2H), 7.58 (s, 1H) 7.61 (s, 1H), 7.75 (d, 2H), 8.25 ppm (d, 2H). <sup>13</sup>C NMR ([d.]DMSO): δ = 21.0, 29.2, 29.5, 123.7, 129.4, 130.5, 131.3, 131.7, 132.3, 133.2, 136.1, 137.2, 138.0, 141.4, 147.0, 188.0 ppm. IR: ν = 1662 (C=O), 1517 and 1344 cm<sup>-1</sup> (NO<sub>2</sub>). MS: *m/z* 351 (M<sup>+</sup> 30%), 336 (100%).

**General procedure for mCBPA oxidations.** A solution of mCPBA (1 mmol for oxidations to sulfoxides; 2.5 mmol for oxidations to sulfones) in CH<sub>2</sub>Cl<sub>2</sub> (5 or 12.5 mL, respectively) was added dropwise, at 0 °C, to a suspension of the sulfide (1 mmol) in dichloromethane (5 mL) and stirred at 25 °C for 16 h. The mixture was diluted with 20 mL dichloromethane and extracted with 10% aqueous Na<sub>2</sub>S<sub>2</sub>O<sub>5</sub>, saturated NaHCO<sub>3</sub> and brine. The organic layer was dried over Na<sub>2</sub>SO<sub>4</sub> and the solvent was removed *in vacuo* to give the crude product that was crystallized from ethanol.



**(3*Z*,5*Z*)-Tetrahydro-3,5-bis-[(4-fluorophenyl)methylene]-4*H*-tetrahydrothiapyran-4-one-1,1-dioxide (1f).** Oxidation of sulfide **3** with 2 eq. mCPBA gave a mixture of sulfone **1f** and the Baeyer-Villiger product **4** which were separated by crystallization from acetone/hexane. **1f** (41 %) had m.p. 179–180 °C. <sup>1</sup>H NMR: δ = 4.43 (s, 4H), 7.12–7.45 (m, 4H), 7.96 ppm (s, 2H). <sup>13</sup>C NMR: δ = 53.1, 116.6 (d, *J*<sub>C-F</sub> = 22 Hz), 126.7 (d, *J*<sub>C-F</sub> = 1 Hz), 129.8 (d, *J*<sub>C-F</sub> = 3 Hz), 132.0 (d, *J*<sub>C-F</sub> = 9 Hz), 143.4, 163.9 (d, *J*<sub>C-F</sub> = 252 Hz), 186.4 ppm. IR: ν = 1664 (C=O), 1333 and 1128 cm<sup>-1</sup> (SO<sub>2</sub>). MS: *m/z* 360 (M<sup>+</sup> 20%), 294 (100%). Elemental analysis calculated (%) for C<sub>19</sub>H<sub>14</sub>F<sub>2</sub>O<sub>3</sub>S: C 63.3, H 3.92, S 8.90. Found: C 63.2, H 3.81, S 8.74. **4** (10%) had m.p. 176–178 °C. <sup>1</sup>H NMR: δ = 4.27 (s, 4H), 6.89 (s, 1H), 7.07–7.14 (m, 4H), 7.53–7.72 (m, 4H), 8.05 ppm (s, 1H). <sup>13</sup>C NMR: δ = 53.1, 55.7, 115.8, 116.13, 116.16, 116.5, 119.9, 128.0, 128.8, 137.4, 126.1, 130.5, 130.6, 131.8, 131.9, 149.7, 162.4, 165.5 ppm. IR: ν = 1721 (C=O), 1315 and 1120 cm<sup>-1</sup> (SO<sub>2</sub>). MS: *m/z* 376 (M<sup>+</sup> 43%), 312 (100%). Elemental analysis calculated (%) for C<sub>19</sub>H<sub>14</sub>F<sub>2</sub>O<sub>4</sub>S: C 60.6, H 3.72. Found: C 60.2, H 3.72.

**(3*Z*,5*Z*)-3-[(4-hydroxyphenyl)methylene]-5-[(4-nitrophenyl)methylene]-4*H*-tetrahydrothiapyran-4-one-1,1-dioxide (1j).** 60% from sulfide **7j**; m.p. 221–224 °C. <sup>1</sup>H NMR ([d<sub>6</sub>]DMSO): δ = 4.68 (s, 4H), 6.87 (d, 2H), 7.46 (d, 2H), 7.70 (s, 1H), 7.77 (d, 2H), 7.84 (s, 1H), 8.29 (d, 2H), 10.22 ppm (broad, 1H). <sup>13</sup>C NMR ([d<sub>6</sub>]DMSO): δ = 51.9, 52.5, 116.0, 123.8, 131.0, 133.0, 138.7, 142.9, 123.7, 124.2, 124.4, 140.4, 147.4, 159.7, 184.0 ppm. IR: ν = 3450 (OH), 1511 and 1349 (NO<sub>2</sub>), 1308 and 1121 cm<sup>-1</sup> (SO<sub>2</sub>). MS: *m/z* 385 (M<sup>+</sup> 5%), 320 (100%).

**(3*Z*,5*Z*)-3-[(4-methoxyphenyl)methylene]-5-[(4-nitrophenyl)methylene]-4*H*-tetrahydrothiapyran-4-one-1,1-dioxide (1k).** 60% from sulfide **7k**; m.p. 158–160 °C (from acetone – hexane). <sup>1</sup>H NMR: δ = 3.88 (s, 3H), 4.35 (s, 2H), 4.51 (s, 2H), 6.99 (d, 2H), 7.42 (d, 2H), 7.58 (d, 2H), 7.98 (s, 1H), 8.02 (s, 1H) 8.32 ppm (d, 2H). <sup>13</sup>C NMR: δ = 52.7, 53.7, 55.5, 114.7, 124.2, 130.2, 132.2, 140.6, 145.2, 123.5, 126.0, 130.0, 140.0, 147.0, 161.6, 185.7 ppm. IR: ν = 1663 (C=O), 1510 and 1346 (NO<sub>2</sub>), 1319 and 1126 cm<sup>-1</sup> (SO<sub>2</sub>). MS: *m/z* 399 (M<sup>+</sup> 10%), 304 (100%).

**(3*Z*,5*Z*)-3-[(4-methylphenyl)methylene]-5-[(4-nitrophenyl)methylene]-4*H*-tetrahydrothiapyran-4-one-1,1-dioxide (1l).** 90% from sulfide **7l**; m.p. 155–158 °C. <sup>1</sup>H NMR: δ = 2.44 (s, 3H), 4.35 (s, 2H), 4.49 (s, 2H), 7.27 (d, 2H), 7.32 (d, 2H), 7.58 (d, 2H), 7.97 (s, 1H), 8.01 (s, 1H) 8.30 ppm (d, 2H). <sup>13</sup>C NMR: δ = 21.6, 52.8, 53.6, 124.2, 125.0, 129.9, 130.0, 130.2, 140.0, 140.8, 141.3, 145.4, 148.2, 185.8 ppm. IR: ν = 1663 (C=O), 1519 and 1346 (NO<sub>2</sub>), 1326 and 1133 cm<sup>-1</sup> (SO<sub>2</sub>). MS: *m/z* 383 (M<sup>+</sup> 20%), 304 (100%).

**(3*Z*,5*Z*)-Tetrahydro-3,5-bis[(4-nitrophenyl)methylene]-4*H*-thiapyran-4-one-1-oxide (2h).** Oxidation of the sulfide **2g** with 1 eq. mCPBA gave a 1 : 1 mixture of sulfone **2g** and sulfoxide **2h** that were separated by flash chromatography on silica gel with 8 : 2 dichloromethane/ethyl acetate as eluent, giving pure **2h** (34%); m.p. 185–190 °C. <sup>1</sup>H NMR: δ = 3.93 (d, 2H, *J* = 12 Hz), 4.21 (d, 2H, *J* = 12 Hz), 7.58 (d, 4H), 8.03 (s, 2H), 8.3 ppm (d, 4H). <sup>13</sup>C-NMR ([d<sub>6</sub>]DMSO): δ = 48.7, 124.3, 131.0, 131.6, 140.8, 141.4, 147.9, 187.0 ppm. IR: ν = 1676 (C=O), 1506 and 1349 cm<sup>-1</sup> (NO<sub>2</sub>). MS: *m/z* 398 (M<sup>+</sup>, 10%), 365 (100%). Elemental analysis calculated (%) for C<sub>19</sub>H<sub>14</sub>N<sub>2</sub>O<sub>6</sub>S: C 57.3, H 3.54, N 7.03, S 8.05. Found: C 57.2, H 3.75, N 7.11, S 7.92.

**(3*Z*,5*Z*)-3,5-Bis[(4-nitrophenyl)methylene]-4-hydroxy-tetrahydro-4*H*-thiapyran-1,1-dioxide (7).** NaBH<sub>4</sub> (0.016 g, 0.44 mmol) was added, in small portions, at 0 °C, with constant stirring, to a solution of **G5** (0.15 g, 0.4 mmol) in 25 mL of a 10 : 1 (v/v) THF/MeOH mixture. After 20 minutes the reaction was quenched by the addition of ice-cold, saturated brine (25 mL) and the product was extracted with diethylether (4 x 25 mL). The combined organic layers were washed with brine, dried over MgSO<sub>4</sub> and the solvent was removed under reduced pressure giving the alcohol **7** (90%): m.p. 216–220 °C. <sup>1</sup>H NMR ((CD<sub>3</sub>)<sub>2</sub>CO): δ = 2.84 (s, 1H), 4.24 (d, 2H), 4.26 (d, 2H), 5.22 (d, 1H), 7.21 (s, 1H), 7.69 (d, 2H), 8.28 ppm (d, 2H). <sup>13</sup>C NMR ((CD<sub>3</sub>)<sub>2</sub>CO): δ = 51.7, 76.7, 123.8, 130.1, 128.5, 134.5, 142.4, 147.3 ppm. IR: ν = 3399 (OH), 1517 and 1351 (NO<sub>2</sub>), 1329 and 1130 cm<sup>-1</sup> (SO<sub>2</sub>). Elemental analysis calculated (%) for C<sub>19</sub>H<sub>16</sub>N<sub>2</sub>O<sub>7</sub>S: C 54.80, H 3.87, N 6.73. Found: C 55.02, H 3.99, N 6.67.

**(3*E*,5*E*)-3,5-Bis[(4-nitrophenyl)methylene]-4-oxocyclohexyl 2,5-dioxo-1-pyrrolidinyl carbonate (8).** *N,N'*-disuccinimidyl carbonate (1.0 g, 3.89 mmol) was added to a solution of **2c** (0.74 g, 1.95 mmol) in 20 mL 1 : 1 dichloromethane/acetonitrile; pyridine was added until the solution became clear (1 mL) and the mixture was stirred at 25 °C for 18 hours. The solution was cooled in an ice bath and the mixed carbonate **8** was precipitated with diethyl ether, filtered and dried (75%). M.p.: 172–175 °C. <sup>1</sup>H NMR ([d<sub>6</sub>]DMSO): δ = 2.71 (s, 4H), 3.30–3.40 (m, 4H), 5.31–5.38 (m, 1H), 7.79 (d, 4H), 7.85 (s, 2H), 8.27 ppm (d, 4H). <sup>13</sup>C NMR ([d<sub>6</sub>]DMSO): δ = 25.3, 32.5, 74.5, 123.6, 131.2, 133.9, 136.7, 141.3, 147.1, 151.0, 169.6, 187.1 ppm. IR: ν = 1810 (C=O), 1788 (C=O), 1740 (C=O), 1670 (C=O), 1518 and 1347 cm<sup>-1</sup> (NO<sub>2</sub>).

**2cPC (9).** *N,N'*-disuccinimidyl carbonate (205 mg, 0.8 mmol) was added to mPEG5000-OH (1.0 g, 0.2 mmol) in a mixture of dry dichloromethane (3.5 mL), acetonitrile (1 mL) and pyridine (0.5 mL) and the solution was stirred

for 18 h at 25 °C, under an argon atmosphere, cooled in an ice bath and the crude product (mPEG-OSu, 94%) was precipitated with diethyl ether, filtered and recrystallized from ethanol. <sup>1</sup>H NMR ([d.]DMSO): δ = 2.80 (s, 4H), 3.30-3.55 (m, PEG), 4.25-4.55 (m, 2H, PEG-CH<sub>2</sub>OSu). 1,3-Diaminopropane (48 μl, 0.57 mmol) and mPEG-OSu (1.0 g, 0.19 mmol), in the minimum amount of dry dichloromethane, were stirred for 18 hours at 25 °C, under an argon atmosphere. The solution was cooled in an ice-bath and the crude mono-PEGylated 1,3-diaminopropane (90 %) was precipitated with diethyl ether, filtered and recrystallized from ethanol. <sup>1</sup>H NMR ([d.]DMSO): δ = 1.48-1.54 (m, 2H, CH<sub>2</sub>), 2.94-2.99 (m, 2H) 3.30-3.55 (m, PEG + CH<sub>2</sub>), 3.98-4.04 (m, 2H, PEG-CH<sub>2</sub>OCONH), 7.17 ppm (m, 1H, NH). Triethylamine was added to a solution of the activated carbonate **8** (0.52 g, 1.0 mmol) and PEGylated 1,3-diaminopropane (1.0 g, 0.2 mmol) in the minimum amount of dry pyridine, to pH 8. The mixture was stirred for 18 h at 25 °C, under an argon atmosphere, and then cooled in an ice bath and the crude product **11** (67 %) was precipitated with diethyl ether, filtered and recrystallized from ethanol. <sup>1</sup>H NMR ([d.]DMSO): δ = 1.35-1.38 (m, 2H), 2.77-2.83 (m, 4H), 3.20-3.70 (m, PEG), 3.97-4.01 (m, 2H), 4.97-5.03 (m, 1H), 7.02-7.09 (m, 2H), 7.74 (d, 4H), 7.77 (s, 2H), 8.30 (d, 4H).

**3-{(3E,5E)-3,5-Bis(*p*-nitrophenyl)methylene}-4-oxocyclohexyloxycarbonyl}propionic acid (**10**). Succinic anhydride (2.63g, 26.3mmol) and DMAP (0.32g, 2.63mmol) were added to a solution of alcohol **2c** (1.0 g, 2.63 mmol) and pyridine (1 mL) in 25 mL 1 : 1 dichloromethane/acetonitrile and the reaction mixture was stirred at room temperature for 16 h and then extracted with 0.1M HCl. The solid emisuccinate (370 mg) was collected while the organic layer was dried over anhydrous sodium sulphate and evaporated. The solid residue was washed with hot methanol giving a second crop of product **10** (664 mg). The crude emisuccinate (82% overall) was used without further purification. M.p.: 195–198 °C. <sup>1</sup>H NMR ([d.]DMSO): δ = 2.31-2.36 (m, 4H), 3.13 (dd, 2H), 3.20-3.25 (m, 2H), 5.14-5.18 (m, 1H), 7.76 (s, 2H), 7.79 (d, 2H), 8.27 (d, 4H), 12.1 ppm (s, 1H). <sup>13</sup>C NMR ([d.]DMSO): δ = 28.8, 32.3, 35.7, 67.0, 123.6, 131.2, 135.0, 135.9, 141.5, 147.0, 171.5, 173.3, 187.0 ppm. IR: ν = 3502 (COOH), 1734 (C=O), 1710 (C=O), 1668 (C=O), 1517 and 1347 cm<sup>-1</sup> (NO<sub>2</sub>). MS: *m/z* 480 (M<sup>+</sup> 8%), 345 (100%).**

**2cPE (11)**. Emisuccinate **10** (0.96 g, 2 mmol), EDC (0.38 g, 2 mmol) and HOBt (0.27 g, 2 mmol) were added, in the order, to mPEG5000-OH (1.0 g, 0.2 mmol) in the minimum amount of dry dichloromethane. Triethylamine was added to pH 8 and the mixture was stirred for 18 h, at 25 °C, under an argon atmosphere. The solution was cooled in an ice bath and the crude product was precipitated by adding diethyl ether, filtered, and recrystallized from ethanol giving 0.76 g of the conjugate **11** (70 %). <sup>1</sup>H NMR ([d.]DMSO): δ = 2.41 (2H), 2.50 (2H), 3.25-3.70 (m, PEG), 3.95-4.00 (m, 2H), 5.13-5.20 (m, 1H), 7.81 (d, 4H), 7.82 (s, 2H), 8.30 ppm (d, 4H).

**Modeling.** Calculations were carried out on a workstation equipped with a Dual Opteron ASUS KFSN4-DRE/IKVM/IST mother board and two AMD Opteron SixCore 2427 2.2 GHz & MB 75W processors. The MMFF94 force field<sup>55</sup> [as implemented in the Spartan'14 parallel suite (Wavefunction inc.)] was used in all energy minimizations. The crystallographic coordinates of the reference covalent complex of phospholipase A2 with paraoxon<sup>46</sup> were obtained from the Protein Data Bank, Brookhaven National Laboratory (Pdb id.: 3D5E). Full details on the construction of the model for the PLA2G7 catalyzed hydrolysis of 2cPE (**11**) are in the Supporting Information.

**Hydrolysis of 2cPE by PLA2G7.** The enzyme (Recombinant Human PLA2G7 from R&D systems, code 5106-PL-010) was added at a final 0.2 nM concentration to a 25mM solution of 2cPE in phosphate buffer, pH7. The reaction was followed by ESI-MS on a Bruker Esquire 400 instrument.

**Biological Assays. Reagents and Antibodies.** The following reagents were used: Bortezomib (LC laboratories), DMSO (Sigma-Aldrich), Resazurin (Invitrogen), GST-Uchl5 (Ubiquigent), ISG15-AMC (BostonBiochem), Ubiquitin-AMC (Ubiquigent), zVAD.fmk (Bachem). Primary antibodies were anti-Actin (Sigma-Aldrich), anti-ubiquitin (Covance) anti-p53 DO-1 (Santa Cruz) anti-Noxa (Merck Millipore).

**Cell culture, cell death and caspase activity.** All cell lines were grown in DMEM supplemented with 10% FBS, penicillin (100U/mL), glutamine (2mmol/L), and streptomycin (100μg/mL) at 37°C in 5% CO<sub>2</sub> atmosphere. In all trypan blue exclusion assays, at least 400 cells from three independent experiments were counted. Data are presented as mean value ± SD. A549 cells engineered to express PLA2G7 were generated by retroviral infection using the pLPC vector and selected for puromycin resistance. The cDNA of PLA2G7 was obtained after retrotranscription of RNAs isolated from A375 cells and PCR amplification using oligonucleotides covering the ORF. The cDNA of PLA2G7 was cloned *blunt/Sall*. Sequencing of the PLA2G7 cDNA was performed to scrutinize for the presence of mutations. The RT-PCR analysis confirming the expression of recombinant PLA2G7 in A549 cells is reported in the Supporting Information.

The caspase activity was evaluated using the Apo-ONE caspase-3/7 homogeneous assay (Promega). The assay includes a profluorescent caspase-3/7 consensus substrate, rhodamine 110 bis-(N-Z-L-aspartyl-L-glutamyl-L-valyl-aspartic acid amide). Cells grown in 96-well plates were treated with the different compounds and tested for caspase activity as recommended by the producer. Data are presented as mean value  $\pm$  SD, n=3.

**Western Blotting.** Tissue and cellular extracts were generated in Laemmli sample buffer. Before lysis, frozen small tissue fragments were pulverized using a dedicated apparatus (TissueLyser Qiagen). Protein extracts, after SDS/PAGE were transferred to a 0.2  $\mu$ m nitrocellulose membrane and incubated with the specific primary antibodies as previously described.<sup>14</sup> After washing, blots were incubated with secondary antibody – peroxidase conjugates (SIGMA). For primary antibody stripping, blots were incubated for 30 min at 60°C in stripping solution (62.5 mM Tris-HCl pH 6.8, 2% SDS, 100 mM  $\beta$ -mercaptoethanol).

**Isopeptidase inhibition.** In a 96-well-plate, 20 nM UCHL1, 20 nM UCHL5, fused to GST, 40 nM His-tagged USP2 catalytic domain or 270 nM USP18 were pre-incubated with G5, **2c** or control for 30 min before substrate Ub-AMC (200 nM) addition. ISG15-AMC (400 nM) was used as substrate for USP18. Reaction buffer was 50 mM Tris pH7.5, 150 mM NaCl, 0.1 mM EDTA, 1 mM DTT. Enzymes relative activities were determined by measuring the RFU values as average of the maximum values obtained within the initial linear range. Enzymatic activities were determined every minute for 60 minutes, at 37 °C. Fluorescence values were read with an Enspire 2300 multilabel reader (excitation 380 nm, emission 460 nm). The RFU values were normalized to 100% of activity for the isopeptidases incubated with vehicle alone. IC<sub>50</sub> were calculated with GraphPad Prism software using a nonlinear fit. Recombinant full-length UCHL1 and USP2 catalytic domain were expressed in bacteria and purified by affinity chromatography using GST or Histidine binding resin, respectively. The human USP18 sequence encoding the region 16-372 corresponding to the translated full-length protein starting at the rare codon CUG was cloned using the Gateway® system in a baculovirus expression vector based on pVL1393 (GE Healthcare). The recombinant protein was expressed in Sf9 insect cells. For protein purification, cells were homogenized (Emulsiflex - Avestin) in lysis buffer (500 mM NaCl, 10% glycerol, 0.01% Tween, 20 mM DTT, 20ug/ml DNaseI, protease inhibitors in 50 mM Na-Phosphate, pH 8.0). Cleared lysates were affinity purified on Gluthatione-sepharose 4B (GE Healthcare) and eluted by cleavage with HRV C3 protease. The protein was then purified on Superdex 200 10/30 GL (GE Healthcare) equilibrated in buffer 500 mM NaCl, 10% glycerol, 5 mM DTT in 50 mM Na-phosphate, pH 8.0. The eluted monomeric protein was concentrated to 3.5 mg/ml and aliquots were flash-frozen in liquid nitrogen. The quality assessment of recombinant protein was performed by ESI LC/MS analysis using a single quadrupole instrument with an electrospray ion source (1100 HPLC G1946 MSD Agilent system).

**Gene expression studies.** Microarray datasets used in this study were downloaded manually from GEO.<sup>43a</sup> We analyzed expression data obtained from GSE48433 (platform HG-U133\_Plus\_2, GPL570 array). We processed all the CEL files together by using standard tools available within the affy package.<sup>56</sup> We used a UniGene ID centered CDF (Chip Description file) in order to have only one intensity value per gene.<sup>57</sup> Details on microarray data processing and analysis are reported in the Supporting Information. The list of lipases was downloaded from Gene Ontology and integrated with HomoloGene; only genes with direct enzymatic activity were considered filtering-out lipases regulators and co-factors. In the end we obtained a list of 173 genes of which 159 were present in the array's platform.

**Statistical analysis.** All assays and control experiments were carried out in triplicate. Results are expressed as means  $\pm$  SD. Statistical analysis was performed by Student's t test and P values  $\leq$  0.05 were considered statistically significant. Asterisks in the figures indicate: \* = P < 0.05; \*\* = P < 0.01; \*\*\* = P < 0.005.

**A549 human lung carcinoma xenograft tumors in mice.** 6-Week-old female athymic nude-foxn1nu (Harlan Ud Italy) were utilized for in vivo xenograft experiments whereas 9-week-old female Balb/C OlaHsd were used for toxicity studies (Harlan Ud Italy). Animal studies were carried out according to the guidelines enforced in Italy (DDL 116 of 21/2/1992 and subsequent addenda) and in compliance with the Guide for the Care and Use of Laboratory Animals, Department of Health and Human Services publication no. 86-23 (National Institutes of Health, Bethesda, MD, 1985). In vivo xenograft tumor model was established from initial s.c. injection of in vitro expanded A549 tumor cells. After tumor mass establishment, solid mass was surgical removed, under sterile conditions, and cut into fragments (2-3 mm), in sterile PBS. Tumor fragments obtained from donor mice were then serially expanded or injected for experimental purpose. 15 mice were implanted s.c with A549 tumor fragments, obtained from donors at passage p8.

**2cPE toxicity analysis.** Animal's body weights were recorded for all animals three times a week from the first day of treatment. All animals were checked daily and eventual behavioral changes, ill health or mortality was recorded for each animal. On day 0, each animal was weighted and the volume of the dose was adjusted to ensure proper dosage in mg/kg. At the end of the experiments mice were sacrificed and basic autopsy was performed on all mice: thoracic and abdominal cavity was open and all major organs were macroscopically examined. Livers from all animals were collected and weighted.

**2cPE administration to mice.** Mice were treated i.v. or s.c., every four days, for three times with 170 mg/kg of **2cPE**, starting from day 16th after tumor fragments injection (day 0), when tumor size was 0.1 cm<sup>3</sup>. Each animal received one dose of 2cEP (170 mg/kg) on day 0, another dose on day 4 and another dose on day 8. For both i.v and s.c, **2cPE** was dissolved in PBS. Injected volume of compound solution was 200  $\mu$ l for each treatment. Control mice received PBS. Before treatment, mice were randomly assigned to experimental groups (n=3 with 4 mice/group). Tumor volume and body weights were recorded for all animals beginning from the day of first treatment and then twice or three times per week, until study termination. The percentage of tumor growth inhibition (TGI) was calculated according to the equation:

$$\%TGI = 100 - \left( \frac{\% TG \text{ Treated group}}{\% TG \text{ Control group}} \times 100 \right)$$

## ASSOCIATED CONTENT

**Supporting Information.** Additional figures illustrating cytotoxic activity, immunoblot analysis of selected markers and 2cPE toxicity; details of animal studies, microarray data processing and analysis, modeling, PLA2G7 catalyzed hydrolysis of **2cPE**; additional analytical and spectral data; HPLC analysis of tested inhibitors. **Compound directory.** SMILES identifiers of compounds discussed in the manuscript. This material is available free of charge via the Internet at <http://pubs.acs.org>.

## AUTHOR INFORMATION

### Corresponding Authors

\*Claudio Brancolini: phone: +39 0432494482; E-mail: [claudio.brancolini@uniud.it](mailto:claudio.brancolini@uniud.it). \*Federico Berti: phone: +390405583920; E-mail: [fberti@units.it](mailto:fberti@units.it).

### Author Contributions

The manuscript was written through contributions of all authors. All authors have given approval to the final version of the manuscript. # U.C. and A.S. contributed equally.

### Notes

The authors declare no competing financial interest.

## ACKNOWLEDGMENTS

This work was supported by AIRC (IG-10437) and FIRB (Progetto RBAP11S8C3\_002) to CB, by the Cross-Border Cooperation Program Italy - Slovenia 2007-2013, by the European Regional Development Fund and national funds to CB and PS, by PRIN (Progetto 20109Z2XRJ\_011) and by the University of Trieste (FRA2013) to FB. AT received a fellowship from AIRC. We thank Cristina Degrossi (MRIT Lab) for assistance with the *in vivo* experiments and Dr. Pierluigi Polese (University of Udine) for the elemental analyses.

## ABBREVIATIONS

BH3, BCL-2 homology domain 3; mCPBA, meta-chloroperoxybenzoic acid; DMAP dimethylaminopyridine; DUBs, deubiquitinating enzymes; EDC, *N*-(3-dimethylaminopropyl)-*N'*-ethylcarbodiimide; GEO, Gene Expression Omnibus; GFP, green fluorescent protein; HDL, high density lipoprotein; HOBt, 1-hydroxybenzotriazole (hydrate); ISG15, interferon-stimulated gene 15; LDL, low density lipoprotein; MPEG500, Poly(ethylene glycol) methyl ether MW 5000; N-SIIs, non-selective isopeptidase inhibitors; PAF-AH, platelet-activating factor acetyl hydrolase; PLA2G7, phospholipase A<sub>2</sub> group 7; SUMO, small ubiquitin-like modifier; TEA, triethylamine; TP53, tumor protein 53; Ub, ubiquitin; Ubl, ubiquitin-like; UCH, ubiquitin carboxy-terminal hydrolase; UPS ubiquitin-proteasome system; USP ubiquitin-specific protease.

## REFERENCES

- (1) Chen, Z. J.; Sun, L. J. Nonproteolytic functions of ubiquitin in cell signaling. *Mol. Cell.* **2009**, *33*, 275–286.
- (2) van der Veen, A. G.; Ploegh, H. L. Ubiquitin-like proteins. *Annu. Rev. Biochem.* **2012**, *81*, 323–357.
- (3) Ciechanover, A.; Stanhill, A. The complexity of recognition of ubiquitinated substrates by the 26S proteasome. *Biochim. Biophys. Acta* **2014**, *1843*, 86–96.
- (4) Satija, Y. K.; Bhardwaj, A.; Das, S. A portrayal of E3 ubiquitin ligases and deubiquitylases in cancer. *Int. J. Cancer* **2013**, *133*, 2759–2768.
- (5) Komander, D.; Clague, M. J.; Urbé, S. Breaking the chains: structure and function of the deubiquitinases. *Nat. Rev. Mol. Cell Biol.* **2009**, *10*, 550 – 563.
- (6) Eletr, Z. M.; Wilkinson, K. D. Regulation of proteolysis by human deubiquitinating enzymes. *Biochim. Biophys. Acta* **2014**, *1843*, 114–128.
- (7) Chen, D.; Frezza, M.; Scmitt, S.; Kanwar, J.; Dou, K. P. Bortezomib as the first proteasome inhibitor anticancer drug: current status and future perspectives. *Curr. Cancer Drug Targets* **2011**, *11*, 239–253.
- (8) Skrott, Z.; Cvek, B. Linking the activity of bortezomib in multiple myeloma and autoimmune diseases. *Crit. Rev. Oncol. Hematol.* **2014**, *9*, 61-70.
- (9) Weathington, N. M.; Mallampalli, R. K. Emerging therapies targeting the ubiquitin proteasome system in cancer. *J. Clin. Invest.* **2014**, *124*, 6–12.
- (10) da Silva, S. R.; Paiva, S. L.; Lukkarila, J. L.; Gunning, P. T. Exploring a new frontier in cancer treatment: targeting the ubiquitin and ubiquitin-like activating enzymes. *J. Med. Chem.* **2013**, *56*, 2165–2177.
- (11) Sgorbissa, A.; Potu, H.; Brancolini, C. Isopeptidases in anticancer therapy: looking for inhibitors. *Am. J. Transl. Res.* **2010**, *2*, 235–247.
- (12) Sippl, W.; Collura, V.; Colland, F. Ubiquitin-specific proteases as cancer drug targets. *Future Oncol.* **2011**, *7*, 619–632.
- (13) Verbitski, S. M.; Mullally, J. E.; Fitzpatrick, F. A.; Ireland, C. M. Punaglandins, chlorinated prostaglandins, function as potent Michael receptors to inhibit ubiquitin isopeptidase activity. *J. Med. Chem.* **2004**, *47*, 2062–2070.
- (14) Aleo, E.; Henderson, C. J.; Fontanini, A.; Solazzo, B.; Brancolini, C. Identification of new compounds that trigger apoptosome-independent caspase activation and apoptosis. *Cancer Res.* **2006**, *66*, 9235–9244.
- (15) Kapuria, V.; Peterson, L. F.; Fang, D.; Bornmann, W. G.; Talpaz, M.; Donato, N. J. Deubiquitinase inhibition by small-molecule WP1130 triggers aggresome formation and tumor cell apoptosis. *Cancer Res.* **2010**, *70*, 9265–9276.
- (16) D'Arcy, P.; Brnjic, S.; Olofsson, M. H.; Fryknäs, M.; Lindsten, K.; De Cesare, M.; Perego, P.; Sadeghi, B.; Hassan, M.; Larsson, R.; Linder, S. Inhibition of proteasome deubiquitinating activity as a new cancer therapy. *Nat. Med.* **2011**, *17*, 1636–1640.
- (17) Coughlin, K.; Anchoori, R.; Iizuka, Y.; Meints, J.; MacNeill, L.; Vogel, R. I.; Orłowski, R. Z.; Lee, M. K.; Roden, R. B.; Bazzaro, M. Small-molecule RA-9 inhibits proteasome-associated DUBs and ovarian cancer in vitro and in vivo via exacerbating unfolded protein responses. *Clin. Cancer Res.* **2014**, *20*, 3174–3186.
- (18) Lee, B. H.; Lee, M. J.; Park, S.; Oh, D. C.; Elsasser, S.; Chen, P. C.; Gartner, C.; Dimova, N.; Hanna, J.; Gygi, S. P.; Wilson, S. M.; King, R. W.; Finley, D. Enhancement of proteasome activity by a small-molecule inhibitor of USP14. *Nature* **2010**, *467*, 179–184.
- (19) Altun, M.; Kramer, H. B.; Willems, L. I.; McDermott, J. L.; Leach, C. A.; Goldenberg, S. J.; Kumar, K. G.; Konietzny, R.; Fischer, R.; Kogan, E.; Mackeen, M. M.; McGouran, J.; Khoronenkova, S. V.; Parsons, J. L.; Dianov, G. L.; Nicholson, B.; Kessler, B. M. Activity-based chemical proteomics accelerates inhibitor development for deubiquitylating enzymes. *Chem. Biol.* **2011**, *18*, 1401–1412.

(20) Reverdy, C.; Conrath, S.; Lopez, R.; Planquette, C.; Atmanene, C.; Collura, V.; Harpon, J.; Battaglia, V.; Vivat, V.; Sippl, W.; Colland, F. Discovery of specific inhibitors of human USP7/HAUSP deubiquitinating enzyme. *Chem. Biol.* **2012**, *19*, 467–77.

(21) Okada, K.; Ye, Y. Q.; Taniguchi, K.; Yoshida, A.; Akiyama, T.; Yoshioka, Y.; Onose, J.; Koshino, H.; Takahashi, S.; Yajima, A.; Abe, N.; Yajima, S. Vialinin A is a ubiquitin-specific peptidase inhibitor. *Bioorg. Med. Chem. Lett.* **2013**, *23*, 4328–4331.

(22) Liang, Q.; Dexheimer, T. S.; Zhang, P.; Rosenthal, A. S.; Villamil, M. A.; You, C.; Zhang, Q.; Chen, J.; Ott, C. A.; Sun, H.; Luci, D. K.; Yuan, B.; Simeonov, A.; Jadhav, A.; Xiao, H.; Wang, Y.; Maloney, D. J.; Zhuang, Z. A selective USP1-UAF1 inhibitor links deubiquitination to DNA damage responses. *Nat. Chem. Biol.* **2014**, *10*, 298–304.

(23) Anchoori, R. K.; Karanam, B.; Peng, S.; Wang, J. W.; Jiang, R.; Tanno, T.; Orłowski, R. Z.; Matsui, W.; Zhao, M.; Rudek, M. A.; Hung, C.; Chen, X.; Walters, K. J.; Roden, R. B. S. A bis-benzylidene piperidone targeting proteasome ubiquitin receptor RPN13/ADRM1 as a therapy for cancer. *Cancer Cell* **2013**, *24*, 791–805.

(24) Foti, C.; Florean, C.; Pezzutto, A.; Roncaglia, P.; Tomasella, A.; Gustincich, S.; Brancolini, C. Characterization of caspase-dependent and caspase-independent deaths in glioblastoma cells treated with inhibitors of the ubiquitin-proteasome system. *Mol. Cancer Ther.* **2009**, *8*, 3140–3150.

(25) Fehnel, E. A.; Carmack, M. Studies in the thiapyran series. The preparation, properties and reactions of 1,4-thiapyrone-1-dioxide. *J. Am. Chem. Soc.* **1948**, *70*, 1813–1817.

(26) Puar, M. S.; Rovnyak, G. C.; Cohen, A. I.; Toeplitz, B.; Gougoutas, J. Z. Orientation of the sulfoxide bond as a stereochemical probe. Thiopyrano[4,3-c]pyrazoles. *J. Org. Chem.* **1979**, *44*, 2513–2518.

(27) Dimmock, J. R.; Padmanilayam, M. P.; Zello, G. a; Nienaber, K. H.; Allen, T. M.; Santos, C. L.; De Clercq, E.; Balzarini, J.; Manavathu, E. K.; Stables, J. P. Cytotoxic analogues of 2,6-bis(arylidene)cyclohexanones. *Eur. J. Med. Chem.* **2003**, *38*, 169–177.

(28) Hansch, C.; Leo, A.; Taft, R. W. A survey of Hammett substituent constants and resonance and field parameters. *Chem. Rev.* **1991**, *91*, 165–195.

(29) Das, U.; Sharma, R. K.; Dimmock, J. R. 1,5-diaryl-3-oxo-1,4-pentadienes: a case for antineoplastics with multiple targets. *Curr. Med. Chem.* **2009**, *16*, 2001–2020.

(30) Dimmock, J. R.; Padmanilayam, M. P.; Puthucode, R. N.; Nazarali, A. J.; Motaganahalli, N. L.; Zello, G. A.; Quail, J. W.; Oloo, E. O.; Kraatz, H. B.; Prisciak, J. S.; Allen, T. M.; Santos, C. L.; Balzarini, J.; De Clercq, E.; Manavathu, E. K. A Conformational and structure-activity relationship study of cytotoxic 3,5-bis(arylidene)-4-piperidones and related N-acryloyl analogues. *J. Med. Chem.* **2001**, *44*, 586–593.

(31) Dimmock, J. R.; Kandepu, N. M.; Nazarali, A. J.; Kowalchuk, T. P.; Motaganahalli, N.; Quail, J. W.; Mykytiuk, P. A.; Audette, G. F.; Prasad, L.; Perjési, P.; Allen, T. M.; Santos, C. L.; Szydłowski, J.; De Clercq, E.; Balzarini, J. Conformational and quantitative structure-activity relationship study of cytotoxic 2-arylidenebenzocycloalkanones. *J. Med. Chem.* **1999**, *42*, 1358–1366.

(32) Dimmock, J. R.; Sidhu, K. K.; Chen, M.; Li, J.; Quail, J. W.; Allen, T. M.; Kao, G. Y. Synthesis and cytotoxic evaluation of some cyclic arylidene ketones and related oximes, oxime esters, and analogs. *J. Pharm. Sci.* **1994**, *83*, 852–858.

(33) Fontanini, A.; Foti, C.; Potu, H.; Crivellato, E.; Maestro, R.; Bernardi, P.; Demarchi, F.; Brancolini, C. The isopeptidase inhibitor G5 triggers a caspase-independent necrotic death in cells resistant to apoptosis: a comparative study with the proteasome inhibitor Bortezomib. *J. Biol. Chem.* **2009**, *284*, 8369–8381.

(34) Tomasella, A.; Blangy, A.; Brancolini, C. A receptor-interacting protein 1 (RIP1)-independent necrotic death under the control of protein phosphatase PP2A that involves the reorganization of actin cytoskeleton and the action of cofilin-1. *J. Biol. Chem.* **2014**, *289*, 25699–25710.

(35) Nicholson, B.; Leach, C. A.; Goldenberg, S. J.; Francis, D. M.; Kodrasov, M. P.; Tian, X.; Shanks, J.; Sterner, D. E.; Bernal, A.; Mattern, M. R.; Wilkinson, K. D.; Butt, T. R. Characterization of ubiquitin and ubiquitin-like-protein isopeptidase activities. *Protein Sci.* **2008**, *17*, 1035–1043.

(36) Liu, Y.; Lashuel, H. A.; Choi, S.; Xing, X.; Case, A.; Ni, J.; Yeh, L. A.; Cuny, G. D.; Stein, R. L.; Lansbury, P. T. Jr. Discovery of inhibitors that elucidate the role of UCH-L1 activity in the H1299 lung cancer cell line. *Chem. Biol.* **2003**, *10*, 837–846.

(37) Sgorbissa, A.; Brancolini, C. IFNs, ISGylation and cancer: cui prodest? *Cytokine Growth Factor Rev.* **2012**, *23*, 307–314.

(38) Potu, H.; Sgorbissa, A.; Brancolini, C. Identification of USP18 as an important regulator of the susceptibility to IFN- $\alpha$  and drug-induced apoptosis. *Cancer Res.* **2010**, *70*, 655–665.

(39) Pasut, G.; Veronese, F. M. State of the art in PEGylation: the great versatility achieved after forty years of research. *J. Controlled Release* **2012**, *161*, 461–472.

(40) Pasut, G.; Veronese, F. M. PEG conjugates in clinical development or use as anticancer agents: an overview. *Adv. Drug Delivery Rev.* **2009**, *61*, 1177–1188.

(41) Safavy, A.; Raisch, K. P.; Mantena, S.; Sanford, L. L.; Sham, S. W.; Krishna, N. R.; Bonner, J. A. Design and development of water-soluble curcumin conjugates as potential anticancer agents. *J. Med. Chem.* **2007**, *50*, 6284–6288.

(42) Kolate, A.; Baradia, D.; Sushilkumar, P.; Vhora, I.; Kore, G.; Misra, A. PEG – A versatile ligand for drugs and drug delivery systems. *J. Controlled Release* **2014**, *192*, 67–81.

(43) a: GEO (Gene Expression Omnibus): <http://www.ncbi.nlm.nih.gov/geo/>; b: HomoloGene: <http://www.ncbi.nlm.nih.gov/homologene>.

(44) Hollingshead, M. G.; Stockwin, L. H.; Alcoser, S. Y.; Newton, D. L.; Orsburn, B. C.; Bonomi, C. A.; Borgel, S. D.; Divilbiss, R.; Dougherty, K. M.; Hager, E. J.; Holbeck, S. L.; Kaur, G.; Kimmel, D. J.; Kunkel, M. W.; Millione, A.; Mullendore, M. E.; Stotler, H.; Collins, J. Gene expression profiling of 49 human tumor xenografts from in vitro culture through multiple in vivo passages--strategies for data mining in support of therapeutic studies. *BMC Genomics*, **2014**, *15*, 393.

(45) Stafforini, D. M.; McIntyre, T. M.; Zimmerman, G. A.; Prescott, S. M. Platelet-activating factor acetylhydrolases. *J. Biol. Chem.* **1997**, *272*, 17895–17898.

(46) Samanta, U.; Nahanson, B. J. Crystal structure of human plasma platelet-activating factor acetylhydrolase – structural implication to lipoprotein binding and catalysis. *J. Biol. Chem.* **2008**, *283*, 31617–31624.

(47) Vijayalakshmi, A.; KrishnaKumari, V.; Madhusudhana, R. N. Probing polyethylene glycol – phospholipid membrane interactions using enzymes. *J. Colloid Interface Sci.* **1999**, *219*, 190–194.

(48) Deslongchamps, P. *Stereoelectronic effects in organic chemistry*; Pergamon Press: Oxford, 1984; pp 54–100.

(49) Berti, F.; Forzato, C.; Nitti, P.; Pitacco, G.; Valentin, E. A study of the enantiopreference of lipase PS (*Pseudomonas cepacia*) towards diastereomeric dihydro-5-alkyl-4- hydroxymethyl-2(3H)-furanones. *Tetrahedron: Asymmetry* **2005**, *16*, 1091–1102.

(50) See for example: (a) Yuhasz S. C., Parry C., Strand M., Amzel L. M., Structural analysis of affinity maturation: the three-dimensional structures of complexes of an anti-nitrophenol antibody. *Mol. Immunol.* **1995**, *32*, 1143–1155. (b) Kleinstein, S. H., Singh, J. P. Why are there so few key mutant clones? The influence of stochastic selection and blocking on affinity maturation in the germinal center. *Int. Immunol.* **2003**, *15*, 871–884 (c) Yang, P. L., Schultz, P. G. Mutational analysis of the affinity maturation of antibody 48G7. *J. Mol. Biol.* **1999**, *294*, 1191–1201.

(51) Andresen, T. L.; Jensen, S. S.; Madsen, R.; Jørgensen, K. Synthesis and biological activity of anticancer ether lipids that are specifically released by phospholipase A2 in tumor tissue. *J. Med. Chem.* **2005**, *48*, 7305–7314.

(52) Andresen, T. L.; Davidsen, J.; Begtrup, M.; Mouritsen, O. G.; Jørgensen, K. Enzymatic release of antitumor ether lipids by specific phospholipase A2 activation of liposome-forming prodrugs. *J. Med. Chem.* **2004**, *47*, 1694–1703.

(53) Rosenson, R. S.; Stafforini, D. M. Modulation of oxidative stress, inflammation, and atherosclerosis by lipoprotein-associated phospholipase A2. *J. Lipid Res.* **2012**, *53*, 1767–1782.



(54) Leonard, N. J.; Choudhury, D.  $\gamma$ -Pyrone by isomerization. Substituted 3,5-dibenzyl-4h-pyran-4-ones. *J. Am. Chem. Soc.* **1957**, *79*, 156–160.

(55) Halgren, T. A. Merck molecular force field. I. Basis, form, scope, parameterization, and performance of MMFF94. *J. Comput. Chem.* **1996**, *17*, 490–519.

(56) Gautier, L.; Cope, L.; Bolstad, B. M.; Irizarry, R. A. Affy-analysis of Affymetrix GeneChip data at the probe level. *Bioinformatics* **2004**, *20*, 307-315.

(57) Dai, M.; Wang, P.; Boyd, A. D.; Kostov, G.; Athey, B.; Jones, E. G.; Bunney, W. E.; Myers, R. M.; Speed, T. P.; Akil, H.; Watson, S. J.; Meng, F. Evolving gene/transcript definitions significantly alter the interpretation of GeneChip data. *Nucleic Acids Res.* **2005**, *33*, e175.